



# **Long-term Trends and Source Apportionment of Particulate Matter (PM<sub>10</sub>) in Auckland**

Louis K. Boamponsem, Philip K. Hopke, Perry K. Davy

February 2025

Technical Report 2025/2







# Long-term trends and source apportionment of particulate matter (PM<sub>10</sub>) in Auckland

February 2025

Technical Report 2025/2

Louis K. Boamponsem

Planning and Resource Consents Department, Auckland Council

Philip K. Hopke

Clarkson University, USA

Perry K. Davy

Institute of Geological and Nuclear Sciences, New Zealand

Environmental Evaluation and Monitoring Unit

Auckland Council

Technical Report 2025/2

ISSN 2230-4525 (Print)

ISSN 2230-4533 (Online)

ISBN 978-1-991146-87-8 (PDF)

The Peer Review Panel reviewed this report
Review completed on 21 February 2025 Reviewed by two reviewers
Approved for Auckland Council publication by: Name: Dr Jonathan Bengé Position: Head of Environmental Evaluation and Monitoring
Name: Jacqueline Lawrence-Sansbury Position: Manager, Air, Land and Biodiversity
Date: 21 February 2025

#### Recommended citation

Boamponsem, L K, P K Hopke, P K Davy (2025). Long-term trends and source apportionment of particulate matter (PM<sub>10</sub>) in Auckland, TR2025/2

#### Cover image credit

Summit of Mount Roskill, Winstone Park, Auckland. Photograph by Luke Harvey

© 2025 Auckland Council, New Zealand

Auckland Council disclaims any liability whatsoever in connection with any action taken in reliance of this document for any error, deficiency, flaw or omission contained in it.

This document is licensed for re-use under the [Creative Commons Attribution 4.0 International licence](#).

In summary, you are free to copy, distribute and adapt the material, as long as you attribute it to the Auckland Council and abide by the other licence terms.



# Executive summary

Airborne particulate matter (PM) and gaseous pollutants pose significant health risks and comprehensive studies on their composition, sources, and trends are needed for effective air quality management. This study investigates the source apportionment of coarse particulate matter (PM<sub>10</sub>) and its long-term trends in Auckland. Over the 2006-2022 study period, consistent decreases in PM<sub>10</sub> concentrations were recorded across the monitored sites, attributed primarily to reductions in motor vehicle emissions facilitated by advancements in fuel formulation and emission control technology.

Five common sources affecting the three PM<sub>10</sub> monitoring sites were resolved using positive matrix factorisation (PMF) receptor modelling. These sources were identified as marine aerosol, motor vehicles, biomass burning, sulphate (primary and secondary), and soil. Marine aerosol contributes substantially to Auckland's PM<sub>10</sub> levels, accounting for over 44 per cent of the mass concentration on average. However, being a natural source, marine aerosol is part of the 'natural' background of Auckland and therefore, a challenge to manage. Marine aerosol contributions showed downward trends over the study period, possibly influenced by changing climate patterns.

Motor vehicles and biomass burning remain the primary anthropogenic sources of PM<sub>10</sub> in Auckland. Biomass burning, particularly during winter months, was a significant contributor to PM<sub>10</sub> concentrations although the use of alternative heating technologies helped stabilise concentrations at two of the three monitored sites. Shipping emissions were identified as having a direct impact on urban air quality with regulations mandating low-sulphur fuels contributing to decreased sulphate source contributions to PM<sub>10</sub>.

This study underscores the importance of ongoing monitoring and emissions reduction strategies, particularly targeting motor vehicles and biomass burning, for enhancing air quality and public health. This research contributes to a broader understanding of PM dynamics in Auckland, informing policy development and air quality management strategies.

# Table of contents

Executive summary .....	iii
Table of contents.....	iv
Table of figures.....	v
List of tables.....	vi
Glossary of terms, acronyms, and abbreviations .....	vii
1 Introduction .....	1
2 Methods .....	3
2.1 PM <sub>10</sub> samples collection, analysis, and sampling sites.....	3
2.2 Data analysis methods .....	6
3 Results and discussion .....	8
3.1 Long-term trends in PM <sub>10</sub> and black carbon concentrations.....	8
3.2 Source apportionment with PMF .....	10
4 Conclusions.....	36
5 References .....	37
6 Acknowledgements.....	46
7 Appendices .....	47
8 Appendix A: PM <sub>10</sub> concentration trends – 2006 to 2022 .....	47
9 Appendix B: PM <sub>10</sub> elemental concentrations box plot.....	48
10 Appendix C: Box plot of all sources identified .....	49
11 Appendix D: Pollution roses for Queen Street .....	50
12 Appendix E. Source profiles time series – Queen Street.....	51
13 Appendix F: Pollution rose for Takapuna site.....	52
14 Appendix G: Source profiles time series – Takapuna site .....	53
15 Appendix H: Pollution roses for Henderson.....	54
16 Appendix I: Source profiles time series plot – Henderson site .....	55
17 Appendix J: Source profiles time series plot – All sites.....	56

## Table of figures

Figure 1. Auckland Council air quality monitoring sites. Takapuna (Lat: -36.7803; Long: 174.7489), Queen Street (Lat: -36.8476; Long. 174.7655), and Henderson (Lat: -36.8676; Long: 174.6282) were selected for the PM <sub>10</sub> source apportionment study. ....	3
Figure 2. Long-term trends in aggregated data from Auckland sites for PM <sub>10</sub> and black carbon pollutants. The plots show the deseasonalised monthly mean concentrations. The solid red line shows the trend estimate and the dashed red lines show the 95% confidence intervals for the trend based on resampling methods. A. PM <sub>10</sub> ; B. Black carbon. All units in µg/m <sup>3</sup> .....	9
Figure 3. Auckland black carbon to PM <sub>10</sub> concentration ratio.....	10
Figure 4. Profiles of the sources resolved by the PMF analysis of the aggregated data collected during 2005- 2022. Top plot: The blue bars are the base values, the unfilled red circle lines are the mean fractional displacement (DISP) values, the asymmetric error bars represent the maximum and minimum DISP values. The filled black circle dots represent the % explained variation.....	14
Figure 5. CBPF plots for marine aerosol and sulphate factors extracted from the aggregated dataset. Wind speeds are in m/s. Values in the parentheses are the 75 <sup>th</sup> percentile values in µg/m <sup>3</sup> .....	15
Figure 6. Long-term trends in the PM <sub>10</sub> source contributions at all the sites. The plot shows the deseasonalised monthly mean concentrations.....	16
Figure 7. Temporal variations in PM <sub>10</sub> source contributions at all sites (the shaded bars are the 95 percentile confidence limits in the mean).....	17
Figure 8. Profiles of the sources resolved by the PMF analysis of the Queen Street site data collected during 2006-2022. Top plot: The blue bars are the base values, the unfilled red circle lines are the mean fractional displacement (DISP) values, the asymmetric error bars represent the maximum and minimum DISP values. The filled black circle dots represent the % explained variation.....	20
Figure 9. CBPF plots for each of the seven factors extracted from the Queen Street site dataset. Wind speeds are in m/s. Values in the parentheses are the 75 <sup>th</sup> percentile values in µg/m <sup>3</sup> .....	21
Figure 10. Long-term trends in the PM <sub>10</sub> source contributions at the Queen Street site. The plot shows the deseasonalised monthly mean concentrations.....	22

Figure 11. Temporal variations in PM <sub>10</sub> source contributions at the Queen Street site (the shaded bars are the 95 percentile confidence limits in the mean).....	23
Figure 12. Profiles of the sources resolved by the PMF analysis of the Takapuna site data collected during 2005- 2022. Top plot: The blue bars are the base values, the unfilled red circle lines are the mean fractional displacement (DISP) values, the asymmetric error bars represent the maximum and minimum DISP values. The filled black circle dots represent the % explained variation.....	25
Figure 13. CBPF plots for each of the seven factors extracted from the Takapuna site dataset. Wind speeds are in m/s. Values in the parentheses are the 75 <sup>th</sup> percentile values in µg/m <sup>3</sup> .....	27
Figure 14. Long-term trends in the PM <sub>10</sub> source contributions at the Takapuna site. The plot shows the deseasonalised monthly mean concentrations.....	28
Figure 15. Temporal variations in PM <sub>10</sub> source contributions at the Takapuna site (the shaded bars are the 95 <sup>th</sup> percentile confidence limits in the mean).....	29
Figure 16. Profiles of the sources resolved by the PMF analysis of the Henderson site data collected during 2006-2022. Top plot: The blue bars are the base values, the unfilled red circle lines are the mean fractional displacement (DISP) values, the asymmetric error bars represent the maximum and minimum DISP values. The filled black circle dots represent the % explained variation.....	30
Figure 17. CBPF plots for each of the seven factors extracted from the Henderson dataset. Wind speeds are in m/s. Values in the parentheses are the 75 <sup>th</sup> percentile values in µg/m <sup>3</sup> . ....	33
Figure 18. Long-term trends in the PM <sub>10</sub> source contributions at the Henderson site. The plot shows the deseasonalised monthly mean concentrations.....	34
Figure 19. Temporal variations in PM <sub>10</sub> source contributions at the Henderson site (the shaded bars are the 95 percentile confidence limits in the mean).....	35

## List of tables

Table 1. Summary of Auckland air quality PM <sub>10</sub> source apportionment monitoring sites: Instruments, Sample Counts, and Sampling Periods .....	5
Table 2. Mean contributions (mass and fractional) of the sources to the observed mass concentrations.....	12



## Glossary of terms, acronyms, and abbreviations

Term	Meaning
Aerosol	A mixture of solid and/or liquid particles suspended in the atmosphere
Air pollutant/contaminant	Any substance in the air that could harm humans, animals, vegetation, or other parts of the environment when present in high enough concentrations
Air pollution	The presence of one or more air pollutants in high enough concentrations to cause harm
Air quality	Air quality is the degree to which air is suitable or clean enough for humans, animals, or plants to remain healthy
Airshed	A geographic area established, as defined by the national environmental standard for air quality (NESAQ), to manage air pollution.
Ambient air	The external air environment (does not include the air environment inside buildings or structures)
Black carbon, BC	Is an air pollutant made up of tiny soot particles discharged into the atmosphere from combustion processes.
BS-DISP	Bootstrap-Displacement. A statistical method used to estimate the uncertainties of the PMF results.
HAPINZ	Health and Air Pollution in New Zealand. The HAPINZ 3.0 study investigated the impact of air pollution on New Zealanders' health. (Kuschel et al. 2022)
Marine aerosol	Particulates emitted from the ocean's surface such as sea salt and byproducts of marine biogenic activity, primarily through the action of wind and waves.
MfE	Ministry for the Environment
Monitoring site	A facility for measuring the concentration of one or more pollutants in the ambient air; also referred to as 'monitoring station'.
NESAQ	National Environmental Standard for Air Quality

Term	Meaning
PM	Particulate Matter. It is made up of a mixture of various sizes of solid and liquid particles suspended in air; a type of air pollutant.
PM <sub>10</sub>	Particulate matter with an aerodynamic diameter of 10 micrometres or less; a type of air pollutant
PMF	Positive Matrix Factorisation. It is a multivariate factor analysis tool that decomposes a matrix of speciated sample data into two matrices: factor contributions and factor profiles.
Pollution rose	A graphic tool used to get a highlight the relationship between wind direction and pollutant concentrations. Generally used to identify directions where there are significant emission sources impacting the measurement site.
Receptor models	Receptor models are mathematical approaches for quantifying the contribution of sources to samples based on the composition or fingerprints of the sources.
SO <sub>2</sub>	Sulphur dioxide, a type of air pollutant.
Stats NZ	Statistics New Zealand
USEPA	United States Environmental Protection Agency
WHO	World Health Organization
µg/m <sup>3</sup>	Microgram of pollutant (1 millionth of a gram) per cubic metre of air, referenced to temperature of 0°C (273.15 K) and absolute pressure of 101.325 kilopascals (kPa).

# 1 Introduction

Air quality is a major environmental issue in urban centres worldwide, with adverse effects on both human health and local visibility (Dehghani et al., 2020; Forouzanfar et al., 2016; Moghadamnia et al., 2017; Tao et al., 2011; Yorifuji et al., 2014; Hu et al., 2020; Pirsahab et al., 2020; WHO, 2021; Stanimirova et al., 2023). The repercussions of compromised air quality span from functional impairments to a spectrum of health symptoms, leading to reduced life expectancy and even death. Globally, air pollution causes over seven million deaths annually (WHO, 2018, 2021; Pirsahab et al., 2020). In New Zealand alone, the societal costs attributed to anthropogenic air pollution in 2016 amounted to \$15.6 billion (Kuchel et al., 2022).

Of the various pollutants degrading air quality, particulate matter (PM) is the most detrimental to human health, with both short- and long-term exposure linked to increased morbidity and mortality rates (Bergamaschi et al., 2007, Smodiš, 2007, Cavanagh et al., 2009, Atkinson et al., 2010, Tobías et al., 2018, de Jesus et al., 2020; WHO, 2021). Global estimates indicate that approximately 4.7 million deaths annually can be attributed to PM exposure (Health Effects Institute, 2024). The detrimental health impacts from PM exposure have been well-documented in numerous epidemiological studies, including immune system reactions, lung irritation, respiratory and cardiovascular diseases, and cancer (Song et al., 2017; Yin et al., 2019; Dai et al. 2021).

PM<sub>10</sub> (particulate matter with aerodynamic diameter  $\leq 10 \mu\text{m}$ ) and PM<sub>2.5</sub> (with diameter  $\leq 2.5 \mu\text{m}$ ) are the metrics used in assessing PM impacts on health (in terms of the burden on individuals, the health system, and society) (Kuchel et al., 2022; Health Effects Institute, 2018; MfE and Stats NZ, 2021; Dehghani et al., 2020; GBD, 2020). Coarser PM typically deposits in the upper airways, while finer PM, penetrates deeper into the lungs (EFCA, 2019; Kuchel et al., 2022).

Particulate matter is a heterogeneous mixture of suspended liquid droplets and solid particles, characterised by variations in size, shape, and chemical composition across space and time (Potukuchi and Wexler, 1995; Pope III et al., 2009; Janssen et al., 2011; Maleki et al., 2021).

Monitoring the mass concentration of air particulate matter alone offers limited insights into the contributing sources. Source apportionment entails the estimation of contributions to airborne pollutants originating from both natural and anthropogenic emissions (Hopke, 2009). Receptor modelling techniques facilitate the estimate of the relative mass contributions from various sources affecting total air particulate matter concentrations (Davy and Trompetter, 2020). The

use of receptor modelling techniques and other appropriate statistical techniques enable the estimation of source contributions through the analysis of elemental concentrations in PM (Davy and Trompetter, 2020; Boamponsem et al. 2024). These analyses can help link policy interventions and economic drivers with changes in pollution source mixes and impacts (Hopke and Hidy, 2022).

The application of receptor models relies on chemical composition and physical data matrices generated from particulate matter samples collected at monitoring sites. There are multiple statistical models and approaches available, such as chemical mass balance (CMB), and positive matrix factorisation (PMF) (Viana et al., 2008 Hopke et al., 2020a). PMF is a powerful and robust tool for source resolution, offering advantages in handling highly time-resolved aerosol composition data with minimal prior knowledge requirements (Ancelet et al., 2012, 2014; Pancras et al., 2013; Moreno et al., 2013; Hovorka et al., 2015; Hopke, 2016; Pokorná et al., 2020). This information can support the building of a complete picture of air quality in Auckland for policy makers to design more effective and efficient regulatory strategies. The findings in this study can also be used in health effects studies to identify those sources most strongly associated with adverse health outcomes (Rich et al., 2019; Croft et al., 2020; Hopke et al., 2020b).

This study's objectives included identifying the sources contributing to PM<sub>10</sub> pollution episodes and tracking source contribution trends over time. This study is part of the largest source apportionment research project in New Zealand to date, providing invaluable insights for both the Auckland region and the entire nation. Building upon a prior publication from this project (Boamponsem et al., 2024), which focused on the source apportionment and trends analysis of PM<sub>2.5</sub> and gaseous pollutants, this paper presents the results of an extensive receptor modelling study utilising PMF on PM<sub>10</sub> samples collected from 2006 to 2022 at three continuous ambient air quality monitoring stations across Auckland.

## 2 Methods

### 2.1 PM<sub>10</sub> samples collection, analysis, and sampling sites

Continuous instrumental monitoring of ambient air quality has been ongoing in the Auckland region for several decades with the Auckland Council amassing data from 1964 to date. These datasets constitute the longest continuous air quality monitoring record in New Zealand.

Auckland's ambient air quality monitoring network comprises 10 permanent sites. These sites have a range in monitoring capabilities representing diverse sources and exposure scenarios, from suburban residential areas to high-traffic locations. While some sites focus on monitoring specific pollutants, others continuously measure a suite of pollutants.

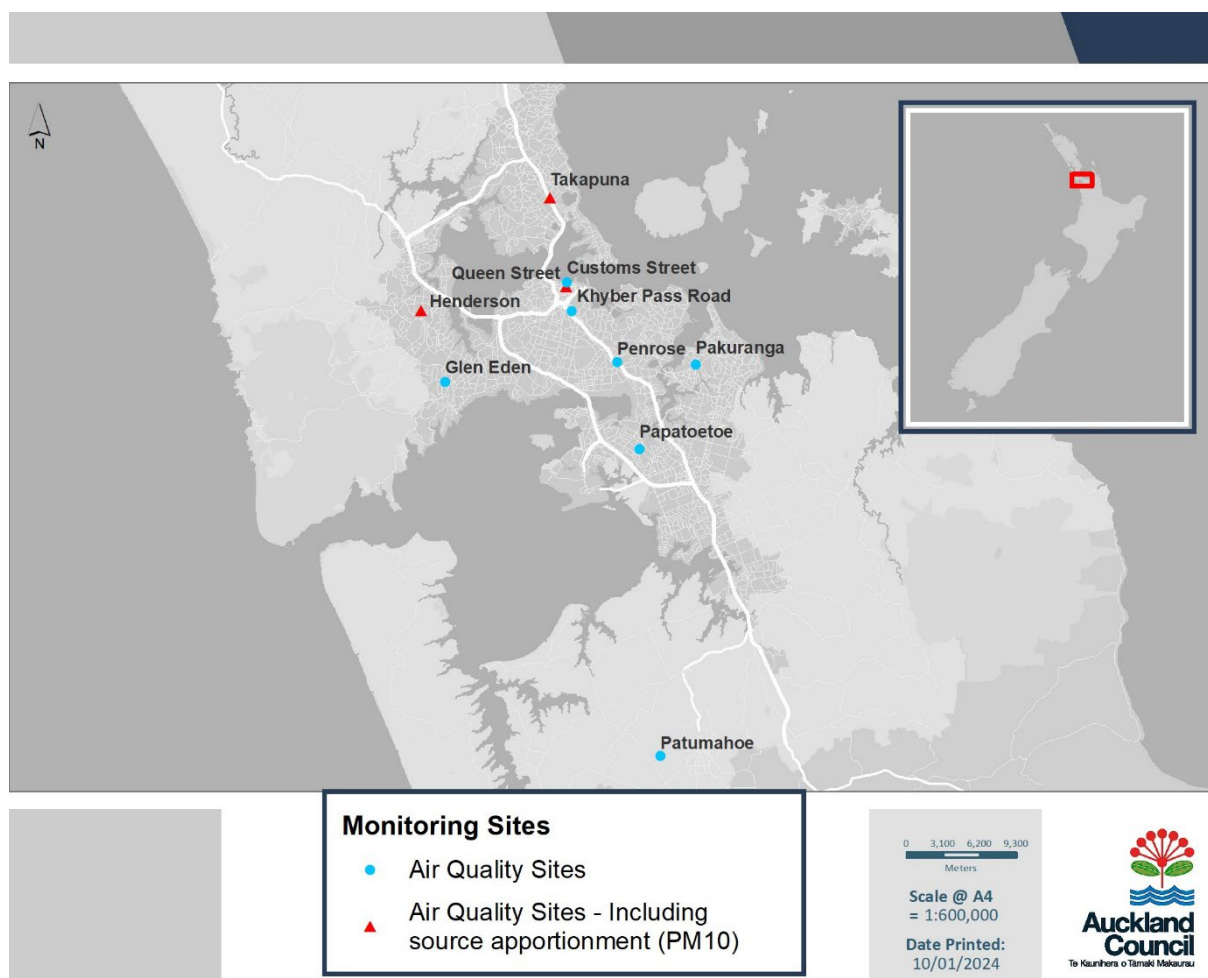


**Figure 1.** Auckland Council air quality monitoring sites. Takapuna (Lat: -36.7803; Long: 174.7489), Queen Street (Lat: -36.8476; Long: 174.7655), and Henderson (Lat: -36.8676; Long: 174.6282) were selected for the PM<sub>10</sub> source apportionment study.

For the source apportionment studies, particulate matter (PM<sub>10</sub>) sampling is ongoing at three monitoring sites: Queen Street, Takapuna, and Henderson. The Queen Street site is situated in the heart of Auckland's city centre, overlooking the primary commercial shopping corridor. The area combines residential apartments, hotels, corporate offices, commercial enterprises and the nearby Port of Auckland. The monitoring station essentially resides within a street canyon aligned north-northeast to south-southwest. Over time, the Queen Street area has undergone numerous changes and upgrades, including alterations to bus routes since 2011, affecting public transport usage. Meteorological conditions at Queen Street are heavily influenced by Auckland central business district's street canyons, with the prevailing wind direction aligned with Queen Street, modified by eddies and turbulence around tall structures.

The Henderson site is located within the grounds of Henderson Intermediate School, on Lincoln Road, Henderson. The site is classed as a suburban site. It is approximately 2km northwest of the Henderson shopping and commercial area. Land use in the area is a mixture of residential and commercial activities with Te Pai Park industrial area (mainly warehousing and light industrial activities) 500m to the northeast and the Waitakere Hospital 300m southeast of the site. The eastern side of the monitoring station is adjacent to Lincoln Road. To the west is the school, and beyond that are residential properties.

The Takapuna site is located approximately 3.5km northwest of the Takapuna shopping and commercial area. The northern side of the monitoring site borders a two-metre mesh fence near Taharoto Road, along the Westlake Girls High School sports field's edge. Approximately 100 metres southeast of the site is a concrete batching plant for ready-mix concrete production. Beyond the immediate surroundings, residential properties extend. The terrain surrounding the Westlake Girls High School site ranges from flat to rolling, with the coastline of the Hauraki Gulf situated three kilometres east. Notably, significant development in the vicinity has occurred over the years, including the redevelopment of school playing fields, the installation of a busway along the northern motorway and the development of the Smales Farm precinct into a bus interchange hub, completed in early 2008 (Davy et al., 2017).

Filter-based (Whatman PTFE 47 mm) PM<sub>10</sub> samples at all sites have been collected since 2005 in at least one site. Queen Street samples were collected daily until 2016 while at the other two sites samples were collected on a 1-day-in-3 basis until 2016. From July 2016 onwards, samples have been collected on a 1-day in-6 basis using Partisol samplers (Rupprecht & Patashnick, Albany, NY,

USA). Summary information regarding data coverage and instruments used for PM<sub>10</sub> sampling can be found in Table 1.

PM<sub>10</sub> concentrations were determined gravimetrically by Watercare Services Limited, and the samples were then forwarded to the New Zealand Ion Beam Analysis Facility, operated by the Institute of Geological and Nuclear Sciences in Lower Hutt, for elemental and black carbon (BC) laboratory analysis. Accelerator based Ion Beam Analysis techniques (PESA, PIXE, PIGE) were used to determine elemental concentrations from Hydrogen (H) and Sodium (Na) to Uranium (U) in the samples while black carbon measurements utilised a M43D Digital Smoke Stain Reflectometer (Edwards et al., 1983; Barry et al. 2012; Trompetter et al. 2005, 2014).

**Table 1.** Summary of Auckland air quality PM<sub>10</sub> source apportionment monitoring sites: Instruments, Sample Counts, and Sampling Periods

Site	PM <sub>10</sub> instrument	Number of Filter Samples	Sample Period
Takapuna*	Thermo 2000H Partisol, 1 in 6 days sampling	1550	Dec 2005 – Dec 2022
Queen Street*	Thermo 2000H Partisol, 1 in 6 days sampling	3709	Jan 2006 – Dec 2022
Henderson*	Thermo 2000H Partisol, 1 in 6 days sampling	1489	Aug 2006 – Dec 2022

\*Takapuna and Henderson were 1-day-in-3 sampling until June 2016, while Queen Street was daily until June 2016

The Ion Beam Analysis was performed using a 3 MeV accelerated proton beam with standards (SrF<sub>2</sub>, NaCl, Cr, Ni, SiO, KCl, and Al) run before and after each analytical cycle. Spectral X-ray peak deconvolution was conducted using Gupix software (Maxwell et al., 1989, 1995). The number of pulses (counts) in each peak for each element is used by the Gupix software to calculate the concentration of that element. The background and neighbouring elements determine the statistical error and the limit of detection. Note that Gupix provides a specific statistical error and limit of detection (LOD) for each element in each particulate matter sample. For further details on

the IBA techniques used, analytical uncertainties and LODs, see previous report by Ancelet et al., (2012).

Meteorological ten-minute average parameters were continuously monitored at the three monitoring sites. Wind speed and direction are real-time measurements obtained with the Vaisala Weather Transmitter WXT520.

## 2.2 Data analysis methods

Receptor modelling analysis of the PM<sub>10</sub> elemental and black carbon datasets was performed using positive matrix factorisation (PMF) with EPA PMF 5.0. PMF is mathematically explained in detail by Paatero and Tapper (1993), Norris et al. (2014), and Hopke (2016).

Detailed explanation of the general PMF principles and terminologies are provided by Norris et al. (2014). The software requires two input matrices, one matrix with the PM<sub>10</sub> elemental concentrations and one with the uncertainties associated with those concentrations. The methodology for developing an uncertainty matrix associated with the elemental concentrations for this work is discussed in detail by Davy et al. (2017). Determination of the number of factors (sources) extracted from the data involved a combination of  $Q_{\text{robust}}$  and  $Q_{\text{theoretical}}$  values, scaled residual distributions, and the physical/chemical interpretation of resulting solutions. Rotational ambiguity was explored through displacement analysis (DISP), and measurement errors were assessed using bootstrap analysis (BS) (Paatero et al., 2014). The source profile plots were generated using a python programming script.

To aid in source identification, the time-series of factor mass contributions and conditional bivariate probability function (CBPF) plots were examined. Conditional bivariate probability function (CBPF) analysis helps to identify wind directions and speeds where high source contributions were likely related. CBPF analysis (Uria-Tellaetxe and Carslaw, 2014) was conducted using the Openair R package (Carslaw and Ropkins, 2012; Carslaw, 2018). Pie charts and box plots were generated using MS Excel and SPSS (version 28).

For the trend analysis of PM<sub>10</sub> and source contributions, the Theil Sen function in Openair R package was used (Carslaw 2012, 2015). The analysis of trends in the PM<sub>10</sub> concentration and source contribution data are accompanied by confidence interval estimates for the observed



trends. Detailed description of the Theil Sen trend method is given by Carslaw (2015). To analyse the overall trends in PM<sub>10</sub> concentration across Auckland spanning from 2006 to 2022, we utilised aggregated data obtained from nine monitoring sites equipped with Beta attenuation monitors (BAM) and T640 PM mass monitors. These sites are Queen Street, Henderson, Takapuna, Penrose, Glen Eden, Pakuranga, Patumahoe, Papatoetoe, and Khyber Pass Road (See Figure 1).

## 3 Results and discussion

### 3.1 Long-term trends in PM<sub>10</sub> and black carbon concentrations

The analysis of the deseasonalised long-term trends in PM<sub>10</sub> concentrations in Auckland, utilising aggregated data from nine air quality monitoring sites (Queen Street, Takapuna, Henderson, Penrose, Khyber Pass Road, Patumahoe, Pakuranga, Papatoetoe, and Glen Eden) found a significant year-on-year reduction of 0.22 µg/m<sup>3</sup> ( $p < 0.001$ ) over the monitoring period from 2006 to 2022. This trend is visually shown by the solid red line in Figure 2A, with upper (-0.17 µg/m<sup>3</sup>/year) and lower (-0.26 µg/m<sup>3</sup>/year), 5% and 95% confidence bounds, respectively, indicated by the hatched lines. All three sites considered for source apportionment in this study indicated a statistically significant decreasing trend (99.9% confidence interval) in PM<sub>10</sub> levels over the monitored period (Appendix A).

Analysing the deseasonalised, long-term trends in PM<sub>10</sub> black carbon concentrations by aggregating data from the three PM<sub>10</sub> source apportionment sites found a year-on-year reduction of 225 ng/m<sup>3</sup> ( $p < 0.001$ ) over the monitored period from 2006 to 2022 (See Figure 2B). This decrease is consistent with the overall decreasing trend in PM<sub>10</sub> levels in Auckland. When the trend in the BC to PM<sub>10</sub> ratio was analysed, it was found that this was decreasing: from approximately 30% in 2006 to 10% in 2022 (See Figure 3). This result is different from the BC/PM<sub>2.5</sub> ratio trend analysis results provided by Boamponsem et al. (2024). Several factors have contributed to the downward long-term trends in PM<sub>10</sub> levels across Auckland. These factors will be discussed in detail as part of the source apportionment results presented and discussed in Section 3.2.

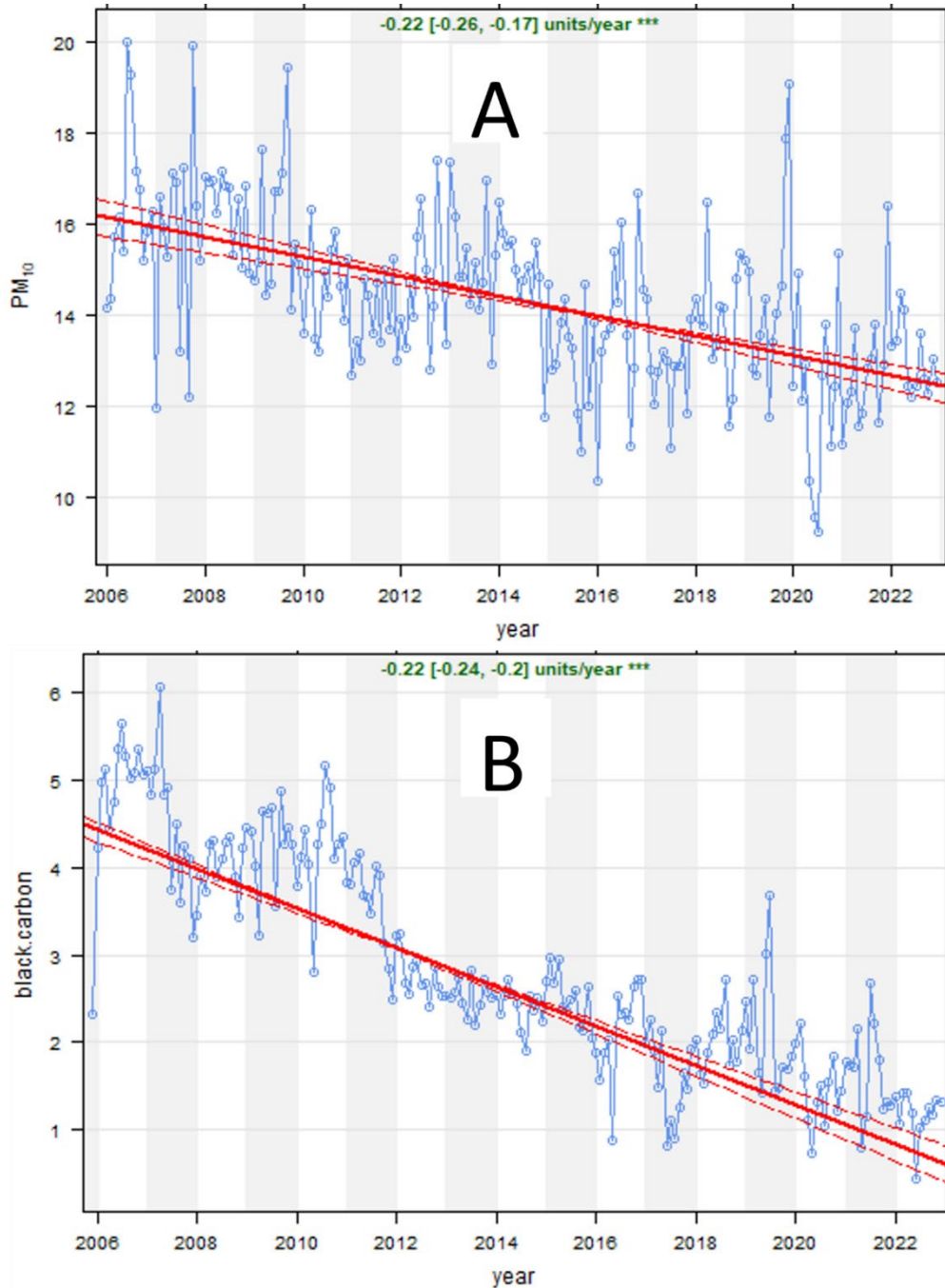


**Figure 2.** Long-term trends in aggregated data from Auckland sites for PM<sub>10</sub> and black carbon pollutants. The plots show the deseasonalised monthly mean concentrations. The solid red line shows the trend estimate and the dashed red lines show the 95% confidence intervals for the trend based on resampling methods. A. PM<sub>10</sub>; B. Black carbon. All units in  $\mu\text{g}/\text{m}^3$ .

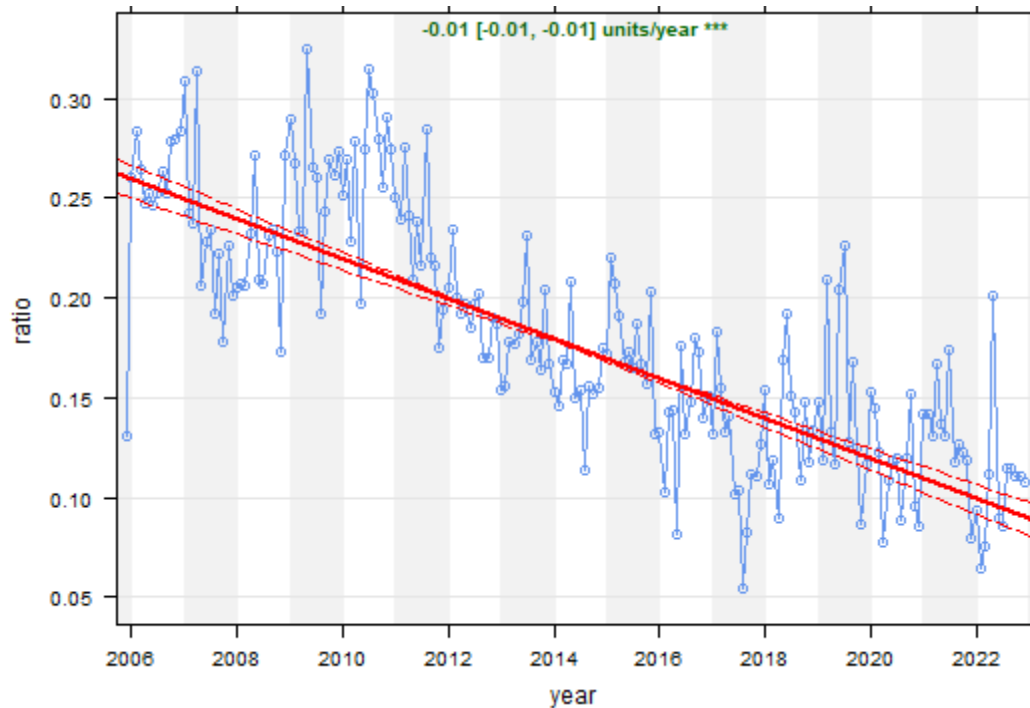


**Figure 3.** Auckland black carbon to PM<sub>10</sub> concentration ratio.

The speciation data provides the opportunity to aggregate the data from all the sites and examine the concentration trends for each individual elemental species as provided by Davy and Trompetter (2021). This result is relevant in terms of the overall environmental loadings originating from air PM<sub>10</sub> emissions. Appendix B presents a box and whisker plot for the key elemental concentrations in the overall PM<sub>10</sub> dataset.

### 3.2 Source apportionment with PMF

Local PM<sub>10</sub> emission sources in Auckland as documented by Davy et al. (2011, 2017, 2020), Boamponsem et al. (2017, 2024), Xie et al. (2019), Crimmins et al. (2019), and Patel (2020, 2024), include:

- Motor vehicles – all roads act as direct sources; the relative contribution of diesel or petrol vehicles to ambient PM loadings at a monitoring site is dependent on the proximity to the nearest road and the relative traffic volume of each vehicle type.
- Local wind-blown soil or road dust sources; dust emissions from road works, construction activities such as new office blocks, apartments, and building refurbishments. Major road works and footpath widening/refurbishment.
- Biomass burning from solid fuel fires used for domestic heating during the winter.
- Port activities – emissions from shipping traffic to and from the Port of Auckland.
- Trans-boundary sources; Australia bush fires and dust storms.
- Marine aerosol (Sea salt).

- Secondary particulate matter resulting from atmospheric gas-to-particle conversion processes (sulphate and nitrate species, organic particle species resulting from photochemical smog events).
- Local commercial/industrial activities – there are a range of light commercial activities (e.g., large brewery, concrete batching plant, quarry, and printing).
- Long-range transport of industrial emissions.
- ‘One-off’ emission events: Fireworks displays and other special events; Short-term, road work and demolition/construction activities.

In the input data statistics provided by the PMF model, signal-to-noise ratio (S/N), calculated by the program for each constituent allows for classification of the element/pollutant as “strong”, “bad” or “weak”. The key source contributors identified for Queen Street, Takapuna, and Henderson sites were found, on average, to explain 99%, 94%, and 93% respectively, of the PM<sub>10</sub> mean gravimetric mass.

The estimated Q values from the PMF solutions were close to the theoretical value for each of the sites. The observed PM<sub>10</sub> concentrations and those calculated from the PMF had a high correlation, and the scaled residual distributions showed good fits to the included species.

Based on the base model, BS, DISP, and BS-DISP from PMF, we found that the solutions were very stable and interpretable, and all factors were mapped in 100% of the 200 bootstrap runs when the five to nine factors were explored depending on the site. All the DISP runs had zero swaps, and there were no swaps in the BS-DISP runs for the best-fit solutions, indicating a stable model solution for each site. For each PMF solution, the PM<sub>10</sub> species and the contributions were normalised using the apportioned PM<sub>10</sub> values in the profiles.

Overall, five unique sources were identified by the PMF analyses as responsible for over 97% of the PM<sub>10</sub> concentrations in Auckland. These sources were motor vehicles, biomass burning, sulphate (primary and secondary), soil, and marine aerosol. It is important to note that commercial and industrial activities can have localised but minor impacts on air quality in Auckland (Boamponsem et al., 2024; Davy et al., 2020). Appendix B and C provide box plots of the elemental concentrations in PM<sub>10</sub> samples and source contribution across the three sites. Table 2 presents the mean contributions (mass and fractional) of the identified sources to the observed PM<sub>10</sub> mass concentrations. The source profiles for each of the three sites and aggregated data are presented by the sections below.

**Table 2.** Mean contributions (mass and fractional) of the sources to the observed mass concentrations.

	Henderson	Takapuna	Queen St	All sites
Mean mass concentrations ( $\mu\text{g m}^{-3}$ )				
PM <sub>10</sub>	13.3	15.2	17.2	15.9
Biomass burning	1.8	1.4	1.5	1.5
Soil	0.9	1.2	1.0	1.0
Motor vehicles	2.1	4.2	5.4	4.4
Marine aerosol	6.2	6.3	7.1	6.7
Sulphate	1.5	1.3	2.1	1.8
Mean % contribution				
Source	Henderson	Takapuna	Queen St	All sites
Biomass burning	14.0	10.0	9.0	10.0
Soil	7.0	8.0	6.0	7.0
Motor vehicles	17.0	29.0	32.0	28.0
Marine aerosol	50.0	44.0	41.0	44.0
Sulphate	12.0	9.0	12.0	11.0

### 3.2.1 All sites combined.

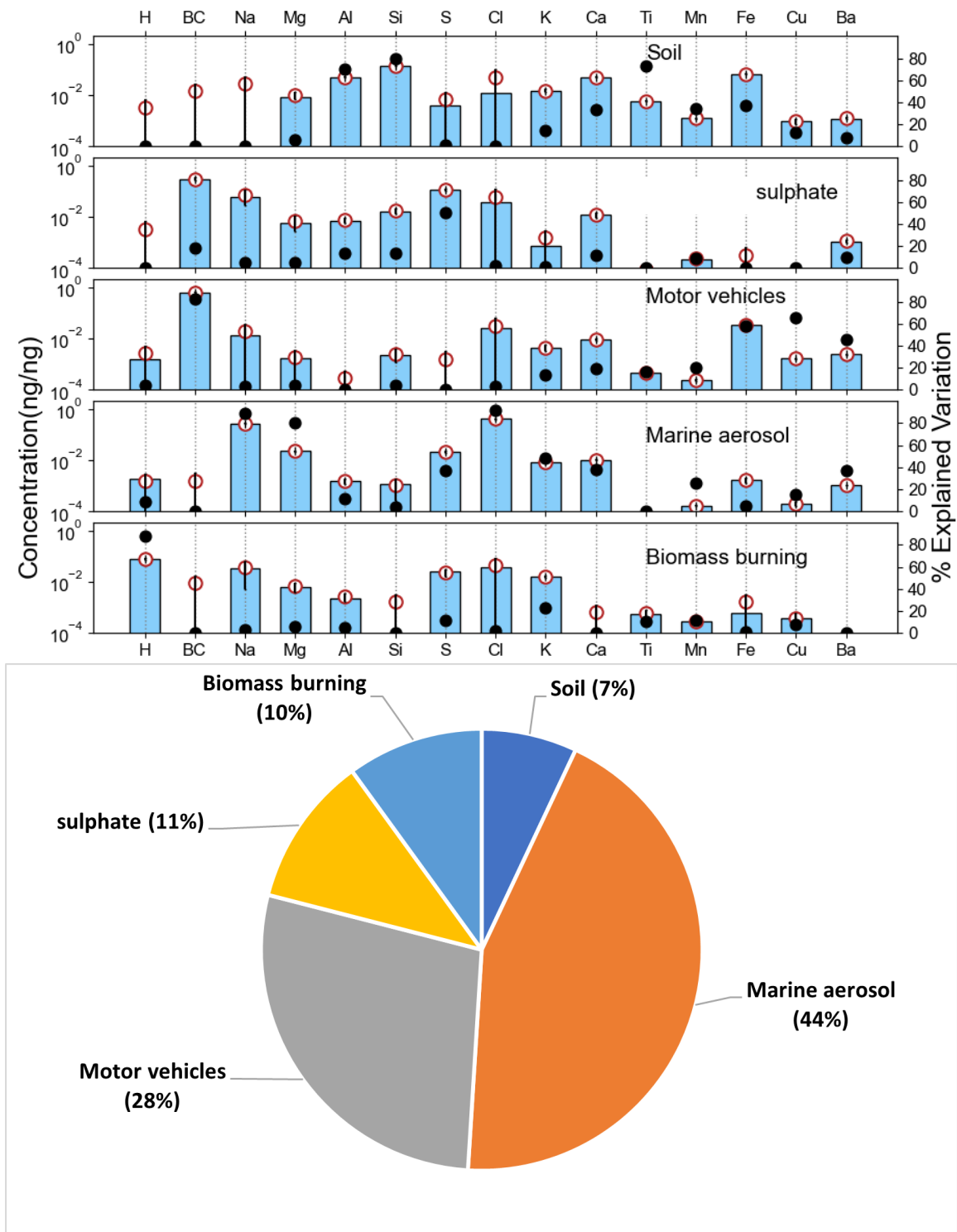
A five-factor PMF solution was resolved for the aggregated data. These factors are marine aerosol, motor vehicles, biomass burning, sulphate (primary and secondary), and soil.

Figure 4 presents the source profiles extracted from the PMF analysis the aggregated data. Time series plot of the sources is given by Appendix J.

Motor vehicles were found to account for 28% of the overall average PM<sub>10</sub> concentration. They primarily contributed to BC, H, Ba, and Cu. There was a downward trend in motor vehicles source contributions over the monitoring period (Figure 6).

Marine aerosol accounted for 44% of the overall PM<sub>10</sub> average mass concentration, with Na and Cl being the dominant species contributed by this source. The PM<sub>10</sub> marine aerosol contribution primarily originated from the southwest, northwest, and northeast directions at higher wind speeds, likely from the Pacific Ocean, Tasman Sea, and Southern Ocean (Figure 5). The contribution of the marine aerosol factor was highest during the spring months and lowest in winter (Figure 7).

Sulphate accounted for 11% of the overall PM<sub>10</sub> average mass concentration, with S being the dominant species contributed by this source. The PM<sub>10</sub> sulphate contribution was found to primarily originate from the northeast sector as shown in Figure 5. Seasonal patterns showed that sulphate source concentrations generally had a summer maximum and a winter minimum (Figure 7). The decreasing trend in sulphate source contributions was consistent with the reduction in sulphur in automotive fuels (6).



**Figure 4.** Profiles of the sources resolved by the PMF analysis of the aggregated data collected during 2005- 2022. Top plot: The blue bars are the base values, the unfilled red circle lines are the mean fractional displacement (DISP) values, the asymmetric error bars represent the maximum and minimum DISP values. The filled black circle dots represent the % explained variation.



Biomass burning was found to be responsible for 10% of the overall PM<sub>10</sub> average concentrations and significantly contributed to BC, and K. Biomass burning had its highest contributions during winter, likely due to both activity (domestic fires for home heating) and meteorological factors such as cold and calm weather. The combined analysis of all the sites indicated an upward trend estimate of 0.04 µg/m<sup>3</sup> per year, with 95% confidence intervals from 0.02 to 0.06 µg/m<sup>3</sup>. The combined trend was statistically significant at the 0.001 level (Figure 6). However, it is worth noting that since 2020, there has been a marked decline in the contribution of biomass burning, which is in line with the increased prevalence of electricity being used for space heating.

Emissions of soil accounted for 7% of the PM<sub>10</sub> data and significantly contributed to the concentrations of Al, Si, Cu, Ca, Si, Ti, Fe, and Mn. These contributions likely resulted from windblown soil, road dust, and dust generated by moving vehicles and road works. There was no significant trend for the soil PM<sub>10</sub> source factor over the monitoring period (Figure 6).

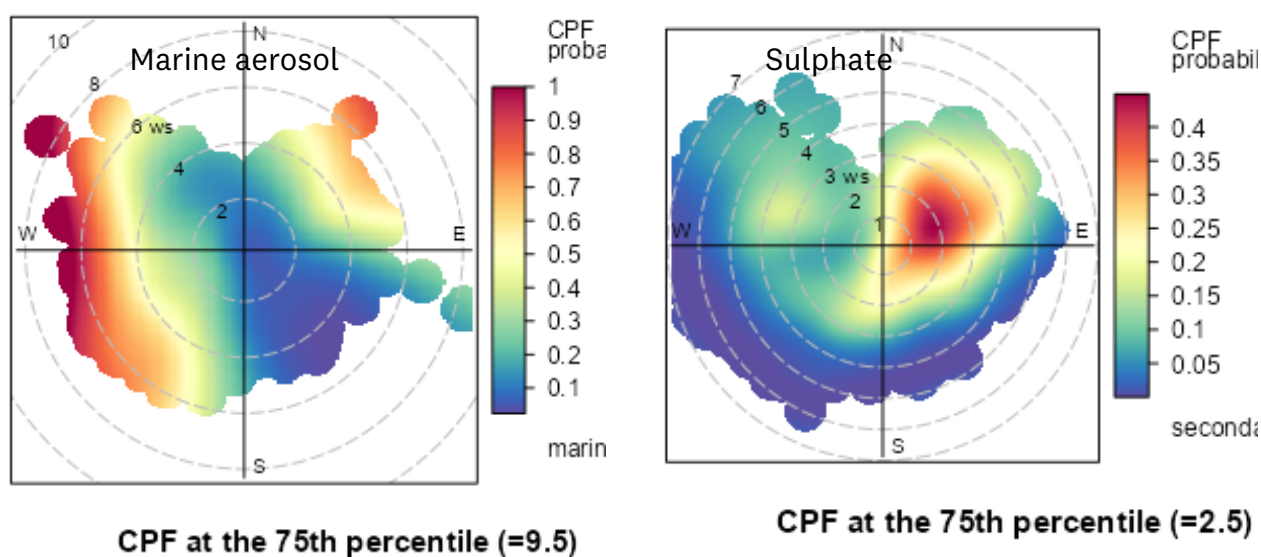


**Figure 5.** CBPF plots for marine aerosol and sulphate factors extracted from the aggregated dataset. Wind speeds are in m/s. Values in the parentheses are the 75th percentile values in µg/m<sup>3</sup>.

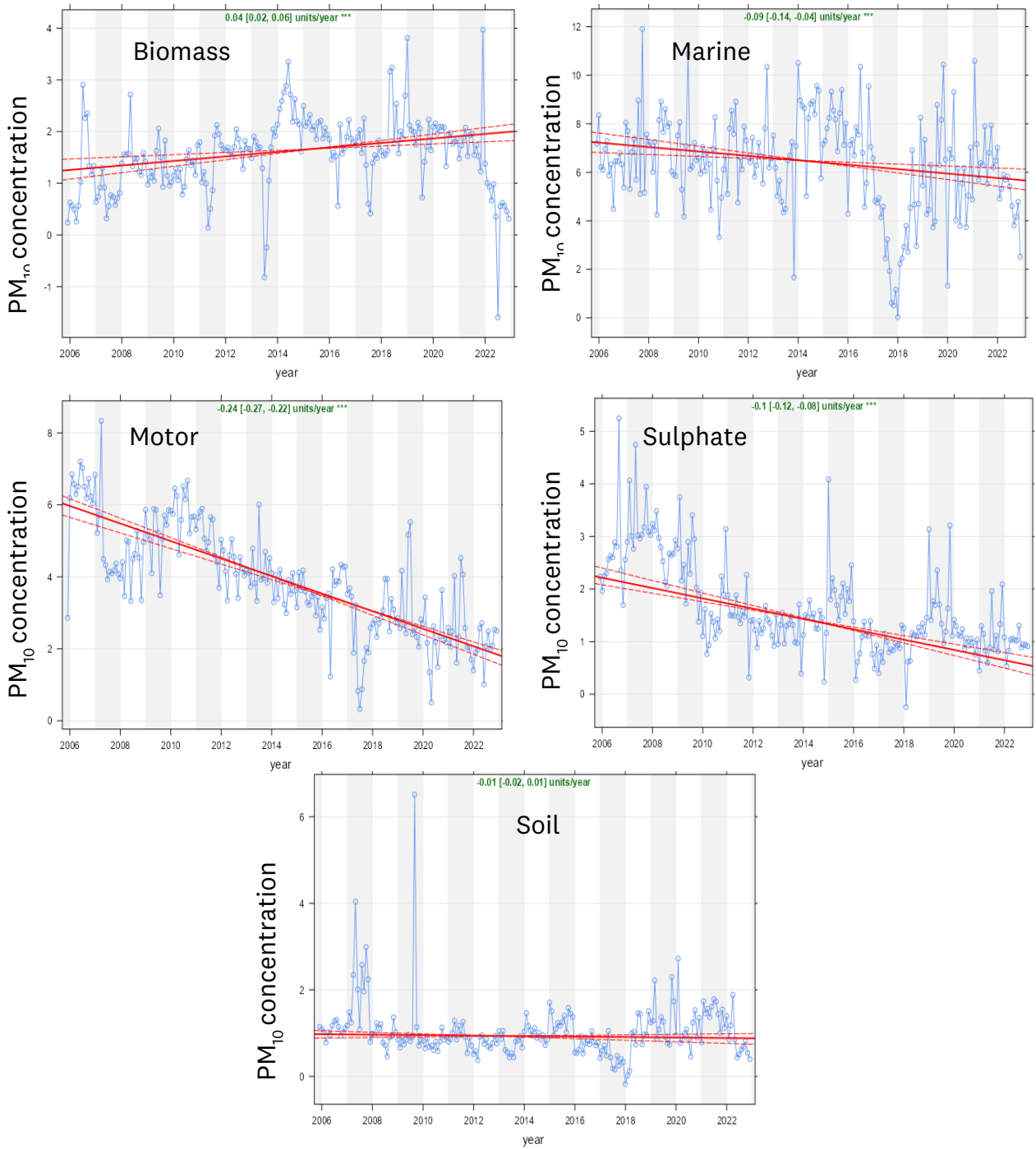


**Figure 6.** Long-term trends in the PM<sub>10</sub> source contributions at all the sites. The plot shows the deseasonalised monthly mean concentrations.

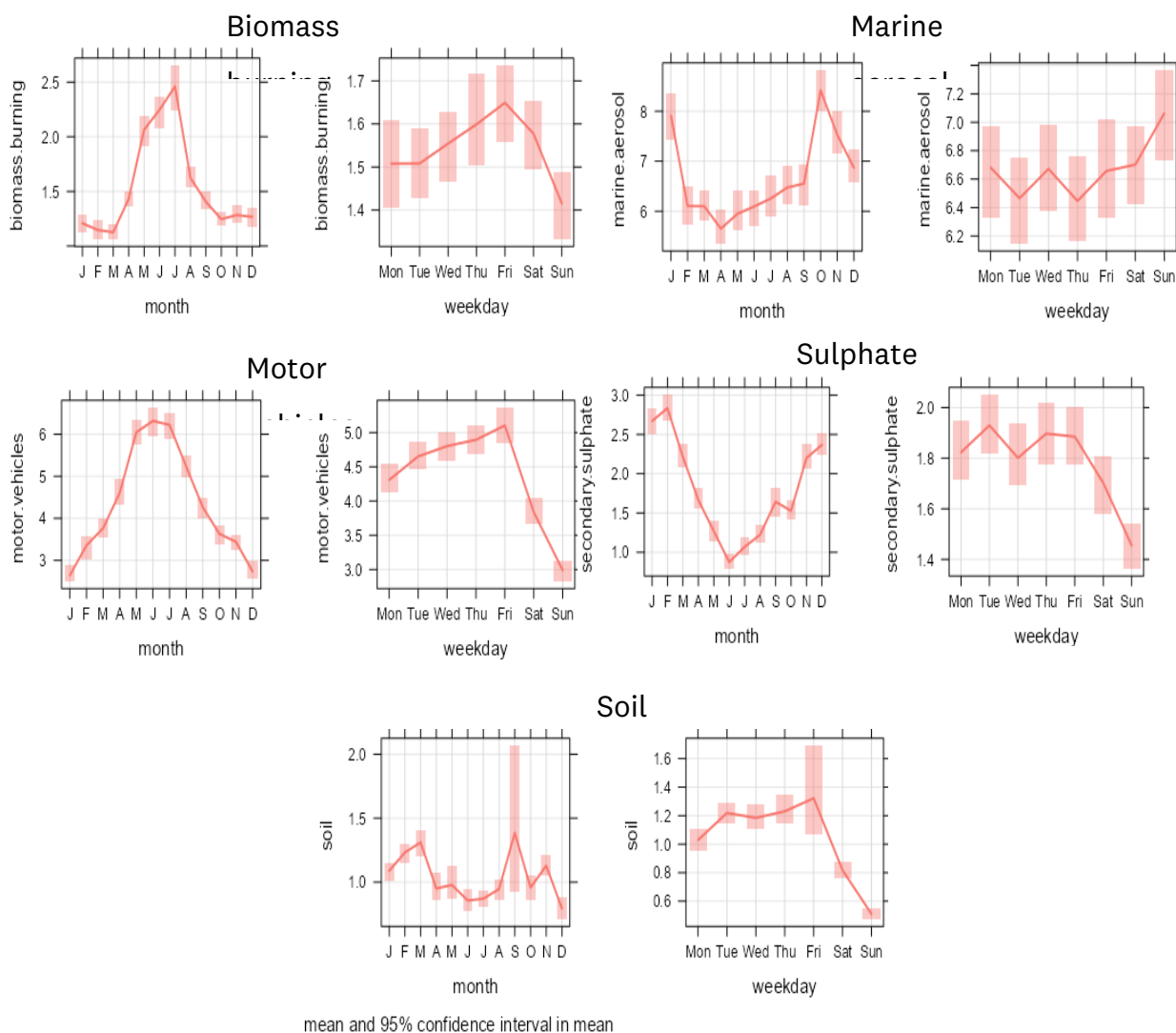


**Figure 7.** Temporal variations in PM<sub>10</sub> source contributions at all sites (the shaded bars are the 95 percentile confidence limits in the mean)

Overall, the data indicates that majority of the observed reduction in PM<sub>10</sub> in Auckland was due to improvements in motor vehicle emissions including the regulated transition to low-sulphur fuels (<10 ppm S for petrol and diesel) despite an overall increase in the number of vehicles on local roads (NZ Ministry of Transport, 2018). The remainder of PM<sub>10</sub> reduction appears to be due a decrease in marine aerosol (sea salt) contributions. Since marine aerosol is a naturally occurring particle, fluctuations in this background source poses a challenge for air quality management.

### 3.2.2 Queen Street site

The selected PMF solution for the Queen Street site resolved five major factors: marine aerosol, motor vehicles, sulphate, biomass burning, and soil. The average source contributions indicated

that marine aerosol and motor vehicle emissions were the most significant contributors to PM<sub>10</sub> concentrations at Queen Street. Figure 8 provides the source profiles extracted from the PMF analysis of Queen Street PM<sub>10</sub> data. Time series plots of the sources are presented in Appendix E. Figure 9 shows the CBPF plots for the sources resolved from the Queen Street data.

Marine aerosol accounted for 41% of the overall PM<sub>10</sub> average mass concentration with sodium (Na) and chloride (Cl) being the dominant species contributing to this source. A significant downward trend in marine aerosol source contributions was observed (Figure 10). It is unclear whether the observed decreasing trend in marine aerosol concentrations is part of a larger inter-decadal cycle related to Southern Hemisphere circulation patterns and atmospheric transport mechanisms or a more permanent trend due to climate change (Davy and Trompetter, 2020). As shown by Figure 11, marine aerosol is more predominant during the summer and spring months due to higher spring equinox winds (Davy et al., 2017).

The emissions from motor vehicles accounted for 32% of the overall average PM<sub>10</sub> concentration and mainly contributed to BC, Fe, Cu, Ti, and Mn concentrations. This profile aligns with previous findings by Davy et al. (2011, 2017) indicating that the motor vehicle emissions exhibit similar characteristics than in previous years. Some trace elements associated with motor vehicle emissions are linked to fuel and oil formulation (e.g., S, Ca, Mg, Na), while others result from engine mechanical wear (Fe) or abrasion of brake linings and road surfaces (e.g., Si, Al, Fe, Cu, Ca, Mg, K, Ti, and Mn) (Amato et al., 2009). Zinc, for example, is emitted by motor vehicles through the combustion of lubricant oils and tire wear and is indicative of stop/start traffic and cold-start engine emissions. Copper, zinc, iron, chromium, and manganese are known to be emitted from road traffic abrasion processes such as brake pad wear (Gianini et al., 2012). A significant downward trend in motor vehicles source contributions over the monitoring period (Figure 10) is attributed to bus route changes, with fewer buses using Queen Street since 2011 due to rerouting of the public transport system.

Sulphate accounted for 12% of the overall PM<sub>10</sub> average mass concentration, with sulphur (S), being the dominant species contributed by this source. Seasonal patterns showed higher sulphate concentrations in summer and lower levels in winter (Figure 11), influenced by solar forcing on atmospheric reaction pathways (Davy et al., 2017, Davy and Trompetter, 2020). There was a decreasing trend in sulphate source contributions attributed to the reduction in sulphur content in automotive fuels as detailed by Davy et al. (2017). Marine diesel emissions of primary sulphate (Agrawal et al., 2008a,b, 2009, 2010) should have been reduced starting in January 2020 due to

the implementation of the International Maritime Organization's rule on the sulphur content of marine diesel fuel reducing it to 0.5% IMO, 2021). It appears that the contributions from this factor did flatten substantially in 2020 (Figure 10). Substantial background concentrations of sulphate are likely due to natural oceanic sources as similar concentrations occur in other New Zealand urban centres (Laura et al., 2024). The highest 25% of PM<sub>10</sub> sulphate contributions primarily originated from the northeastern sectors (Figure 9), likely due to ship emissions from the Port of Auckland and Hauraki Gulf shipping lanes. Previous reports by Davy et al. (2017, 2020) found that emissions from ships entering and exiting the Port of Auckland are a primary source of sulphate.

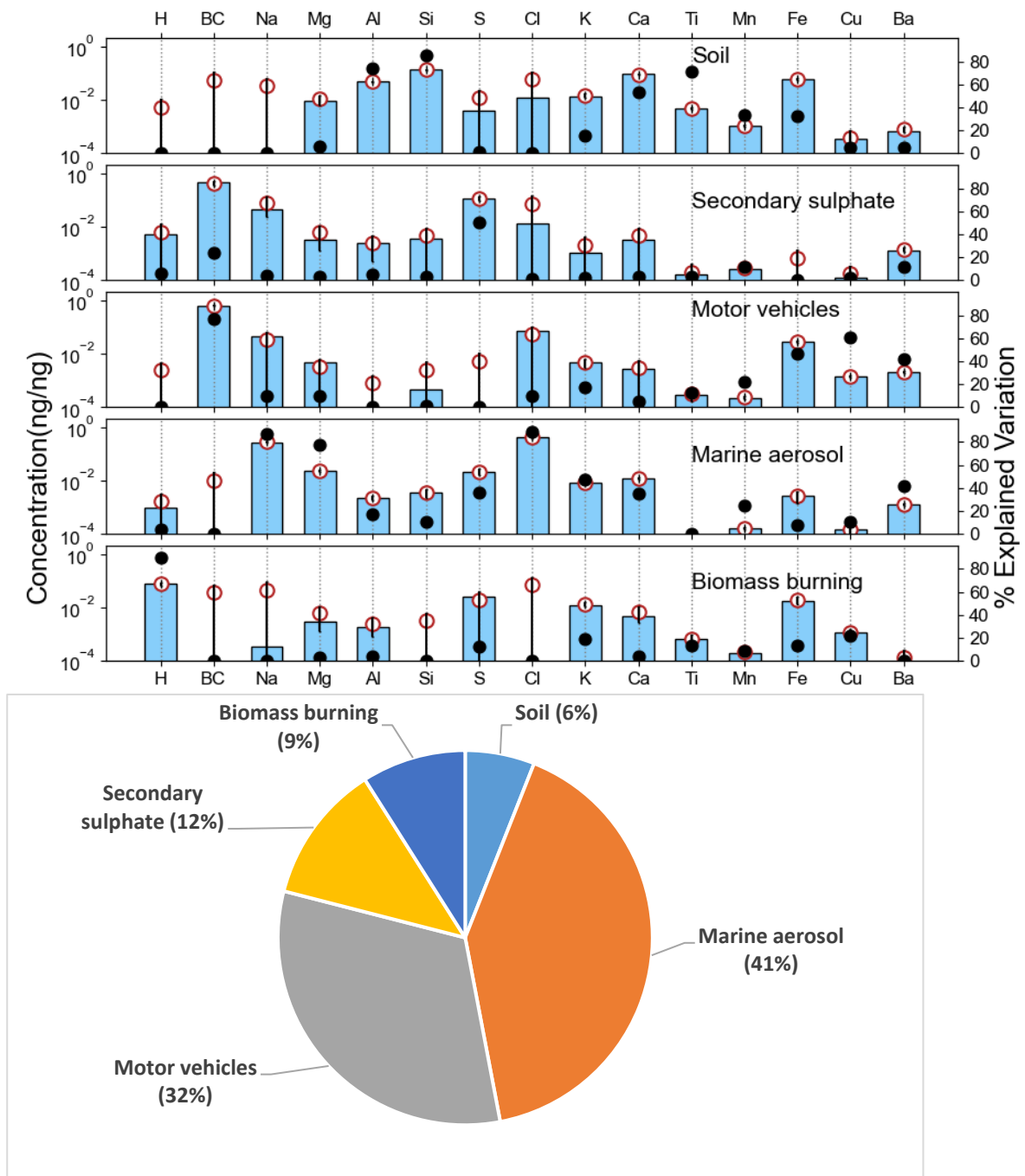


**Figure 8.** Profiles of the sources resolved by the PMF analysis of the Queen Street site data collected during 2006-2022. Top plot: The blue bars are the base values, the unfilled red circle lines are the mean fractional displacement (DISP) values, the asymmetric error bars represent the maximum and minimum DISP values. The filled black circle dots represent the % explained variation.

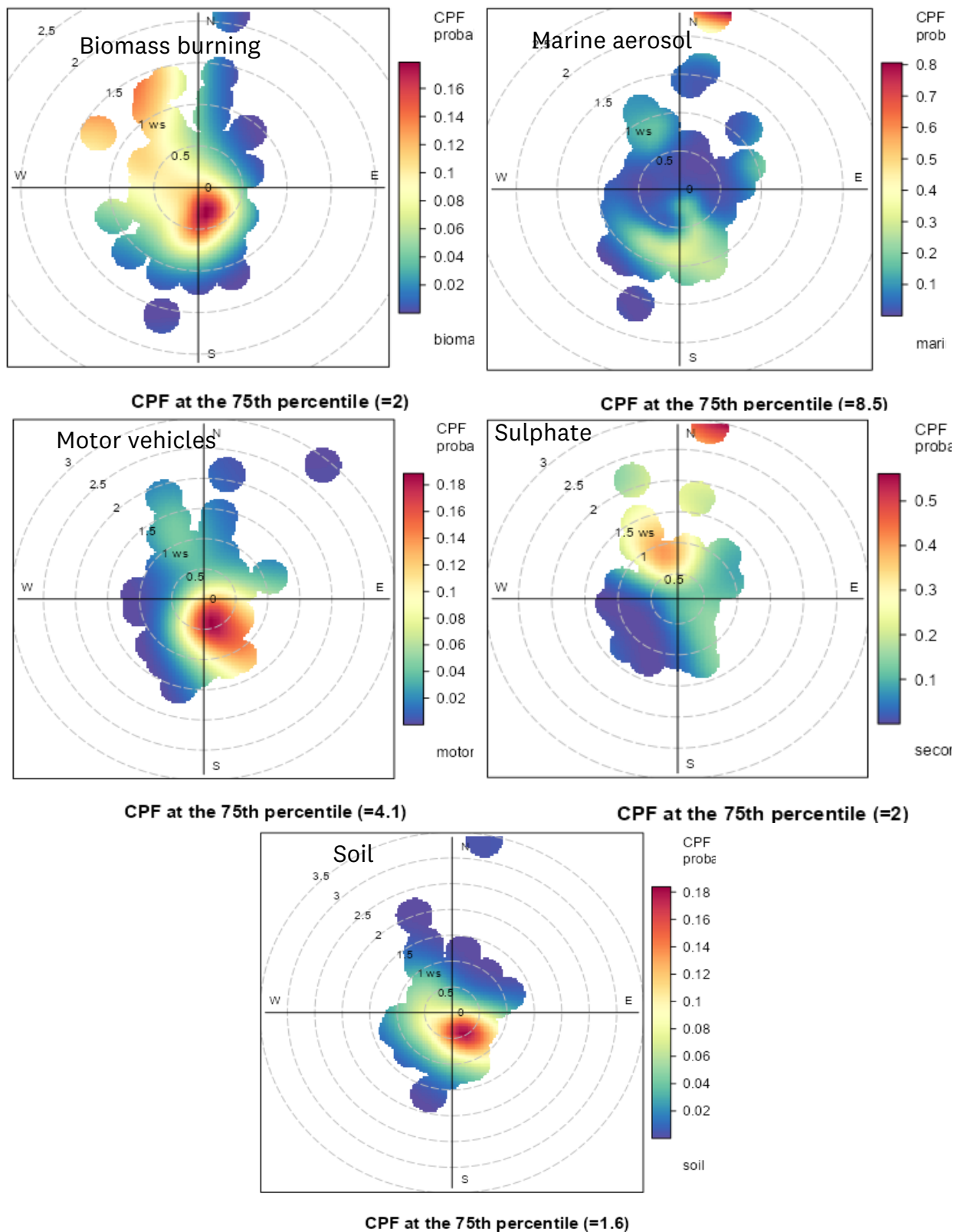


**Figure 9.** CBPF plots for each of the seven factors extracted from the Queen Street site dataset. Wind speeds are in m/s. Values in the parentheses are the 75<sup>th</sup> percentile values in  $\mu\text{g}/\text{m}^3$ .

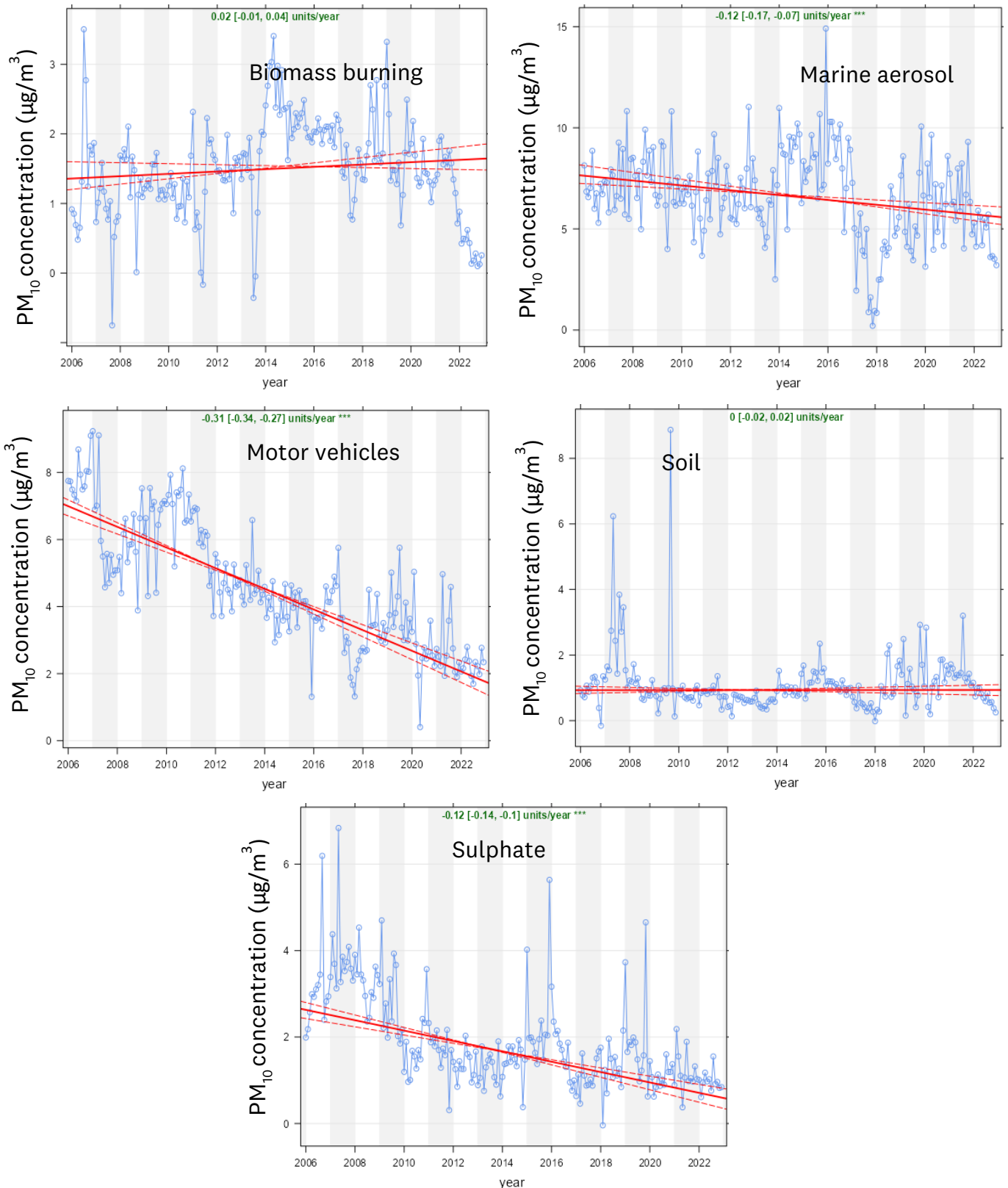


**Figure 10.** Long-term trends in the PM<sub>10</sub> source contributions at the Queen Street site. The plot shows the deseasonalised monthly mean concentrations.



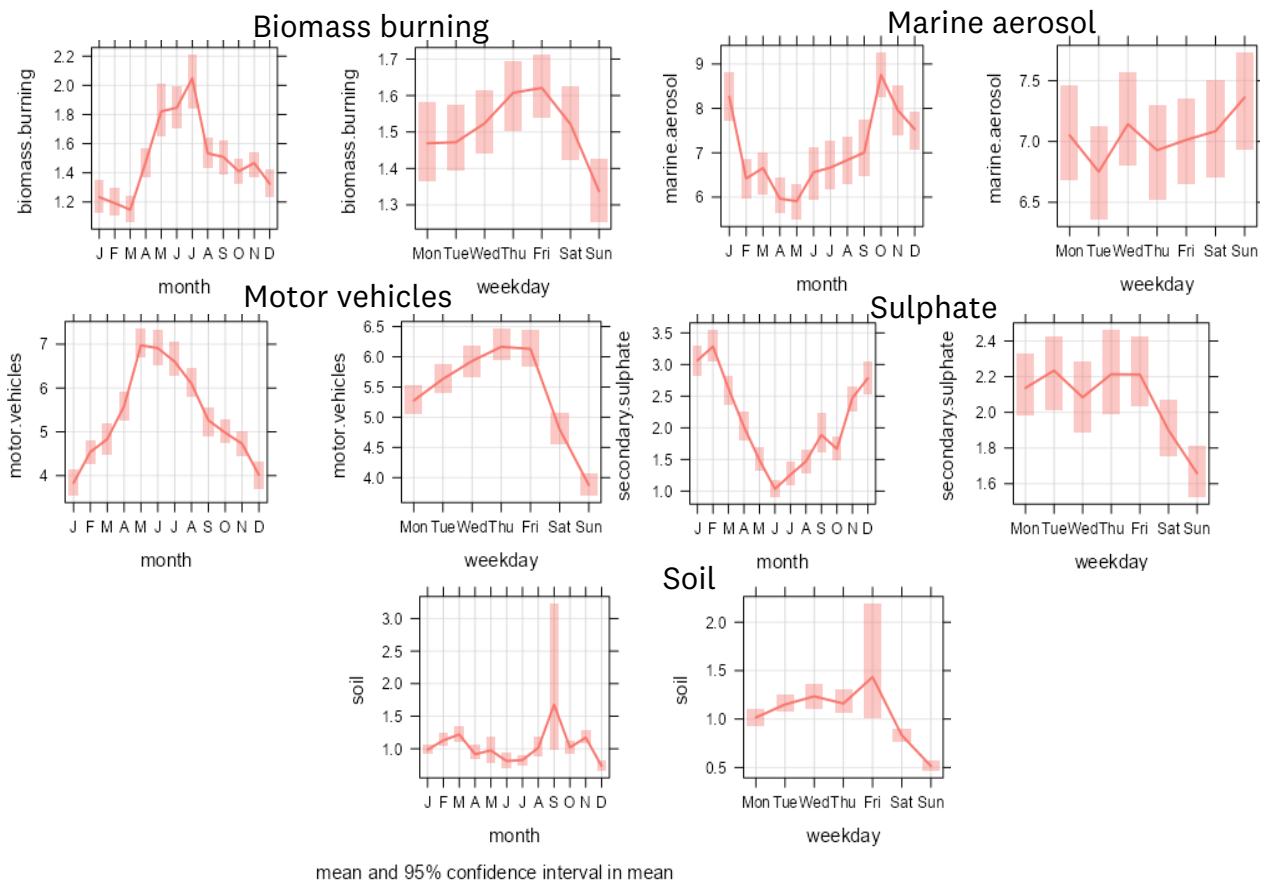


**Figure 11.** Temporal variations in PM<sub>10</sub> source contributions at the Queen Street site (the shaded bars are the 95 percentile confidence limits in the mean).

Biomass burning contributed 9% to the overall average PM<sub>10</sub> concentrations and significantly contributed to hydrogen (H; marker of organic carbon), and potassium (K). Potassium is a commonly used marker element for biomass combustion, while Davy et al have shown that elevated concentrations of arsenic occur every winter in many New Zealand urban areas as a result of the use of copper chrome arsenate treated timber as fuel for domestic space-heating appliances (Davy et al 2014). Particles from biomass burning in Auckland’s CBD likely originate from surrounding suburbs (Figure 9), with peak contributions during winter due to emissions from solid fuel fires for domestic heating in neighbouring residential areas. Like in the PM<sub>2.5</sub> source apportionment results (Boamponsem et al. 2024), there is no significant trend observed for the biomass burning source factor (Figure 10). According to census results and home heating surveys, despite the increasing number of households in Auckland, there has been a decline in the number of households using solid fuel for home heating (Metcalf et al. 2018). The last three New Zealand Censuses have included a question regarding the methods used to provide heat for households. In 2013, 21% of Auckland households stated that the combustion of wood was a heating method

used, a fall from 30% of households recorded in the 2001 census (Statistics New Zealand, 2014). Efficient heat pump electrical heating options are becoming increasingly common for the main living areas throughout Auckland as the proportion of dwellings burning wood, coal, and liquefied petroleum gas (LPG) declines (Stones-Havas, 2014; Statistics New Zealand, 2014; Crimmins, 2017).

Emissions of soil accounted for 6% of the PM<sub>10</sub> data and substantially contributed to the concentrations of aluminium (Al), silicon (Si), titanium (Ti), iron (Fe), and manganese (Mn). This source includes windblown soil, road dust, and dust generated by moving vehicles and road works (Davy et al., 2011). Figure 11 suggests that the soil source is primarily anthropogenic since it has a weekday/weekend concentration difference. The trends in soil are influenced by significant road work activity on Queen Street during 2007-2008, decreasing afterward (Figure 10).

### **3.2.3 Takapuna site**

The PM<sub>10</sub> pollution rose at the Takapuna site shows the highest concentrations from the southwestern quarter where SH1 is located relative to the site (Appendix F). A five-factor PMF solution was also resolved for the Takapuna site. These factors are marine aerosol, motor vehicles, biomass burning, sulphate, and soil. Figure 12 presents the source profiles extracted from the PMF analysis of Takapuna PM<sub>10</sub> data. Time series plot of the sources is given in Appendix G.

Marine aerosol accounted for 44% of the overall PM<sub>10</sub> average mass concentration, with Na and Cl being the dominant species contributed by this source. The Takapuna PM<sub>10</sub> marine aerosol contribution mainly originated from the west and northeast directions (Figure 13). In line with the Queen Street and Henderson sites, a downward trend in marine aerosol source contributions was observed at the Takapuna site (Figure 14). The most likely source of the PM<sub>10</sub> marine aerosol is the Southern Ocean, Tasman Sea, and Pacific Ocean. Like the other sites, the contribution of the marine aerosol factor was highest during the spring months and lowest in winter (Figure 15).

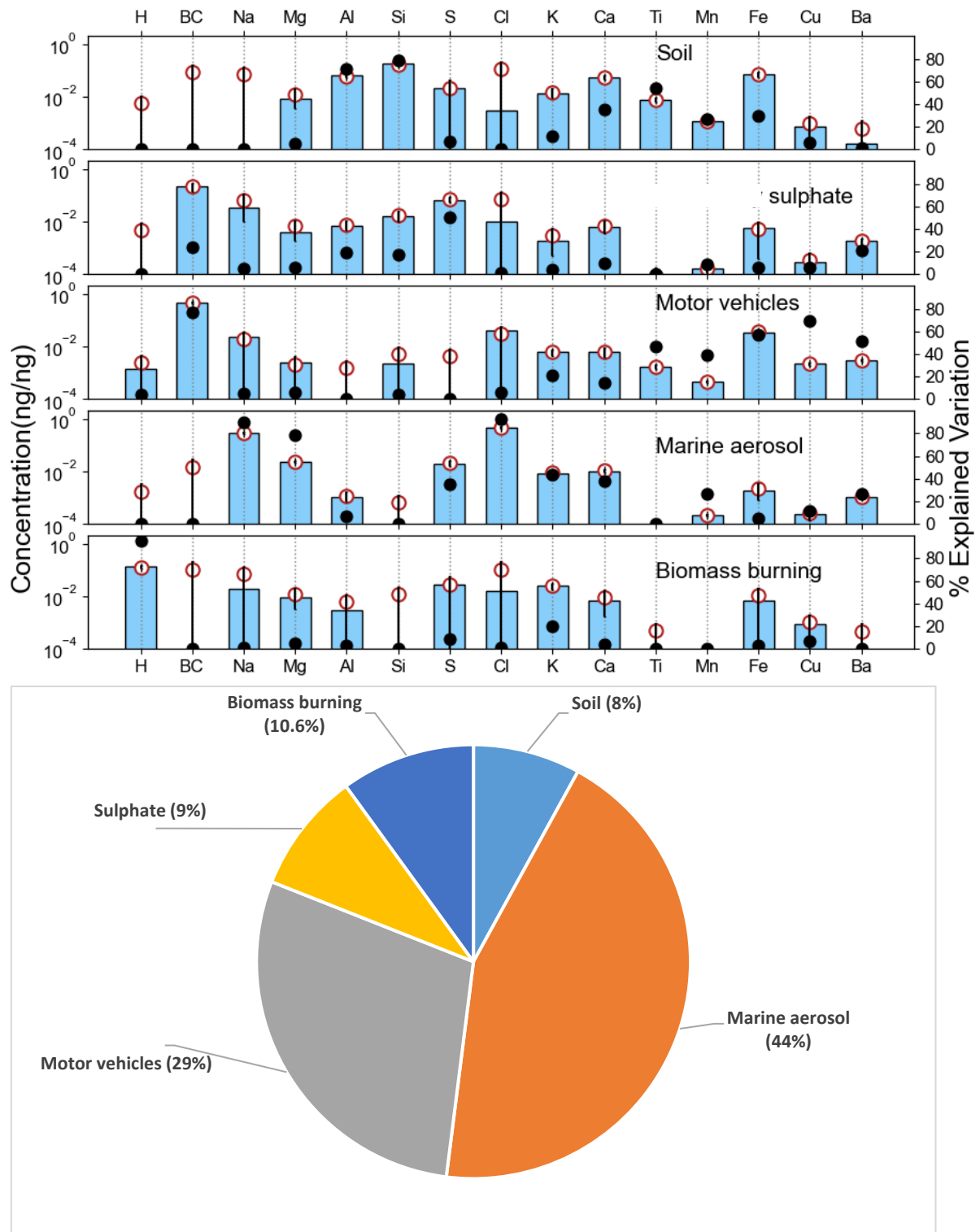


**Figure 12.** Profiles of the sources resolved by the PMF analysis of the Takapuna site data collected during 2005- 2022. Top plot: The blue bars are the base values, the unfilled red circle lines are the mean fractional displacement (DISP) values, the asymmetric error bars represent the maximum and minimum DISP values. The filled black circle dots represent the % explained variation.

Motor vehicles were found to account for 29% of the overall average PM<sub>10</sub> concentration. This source primarily contributed to BC, Ti, Fe, Cu, Mn, and Ba. As with other sites, the higher motor vehicle source contribution in winter is consistent with colder months and less efficient combustion. The motor vehicle source for PM<sub>10</sub> shows a westerly direction for peak concentrations as presented below and is likely to be due to traffic on the nearby motorway. As with other sites, there was a downward trend in motor vehicles source contributions that is statistically significant at the 0.05 level (Figure 14).

Sulphate accounted for 9% of the overall PM<sub>10</sub> average mass concentration, with sulphur as the key source indicator species contributed by this source. The highest proportion of PM<sub>10</sub> sulphate contributions primarily originated from the northeastern sector (Figure 13). The decreasing trend in sulphate source contributions was consistent with other sites (Figure 14). Seasonal patterns showed that sulphate source contributions generally had a summer maximum and a winter minimum (Figure 15).

Biomass burning was found to be responsible for 10% of the overall PM<sub>10</sub> average concentrations and significantly contributed to the total mass concentration of BC, and K. Particles from biomass burning at Takapuna are considered to originate residential solid fuel combustion from Takapuna and surrounding suburbs. As with other sites, biomass burning had its highest contributions during winter, likely due to both activity (domestic fires for home heating) and meteorological factors such as cold and calm weather. There was a significant upward trend in biomass burning source contributions until 2020 followed by a marked decrease in recent years (Figure 14). These changes indicate a need for further investigation on the changes experienced by this area of Auckland in the recent past.

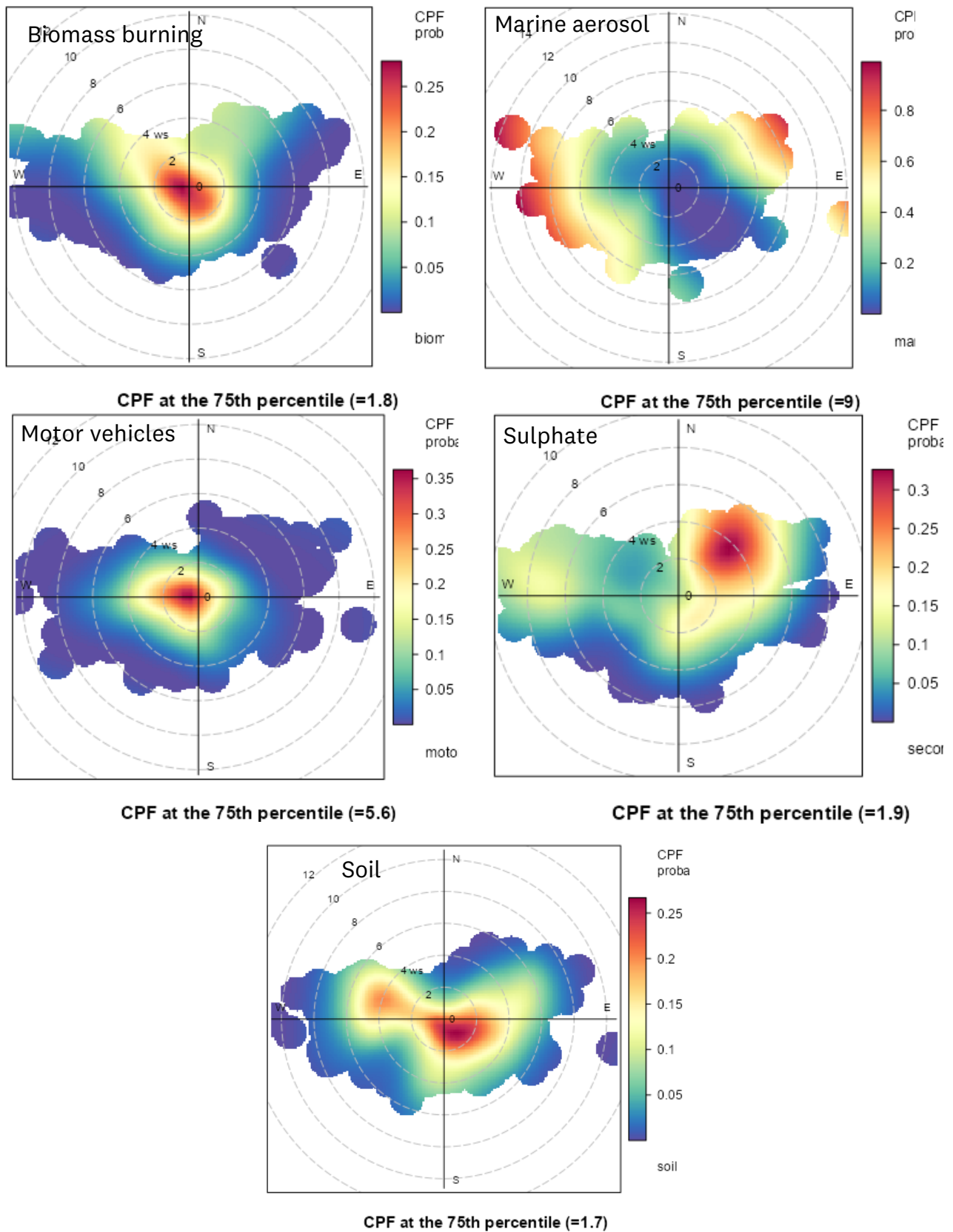


**Figure 13.** CBPF plots for each of the seven factors extracted from the Takapuna site dataset. Wind speeds are in m/s. Values in the parentheses are the 75<sup>th</sup> percentile values in  $\mu\text{g}/\text{m}^3$ .

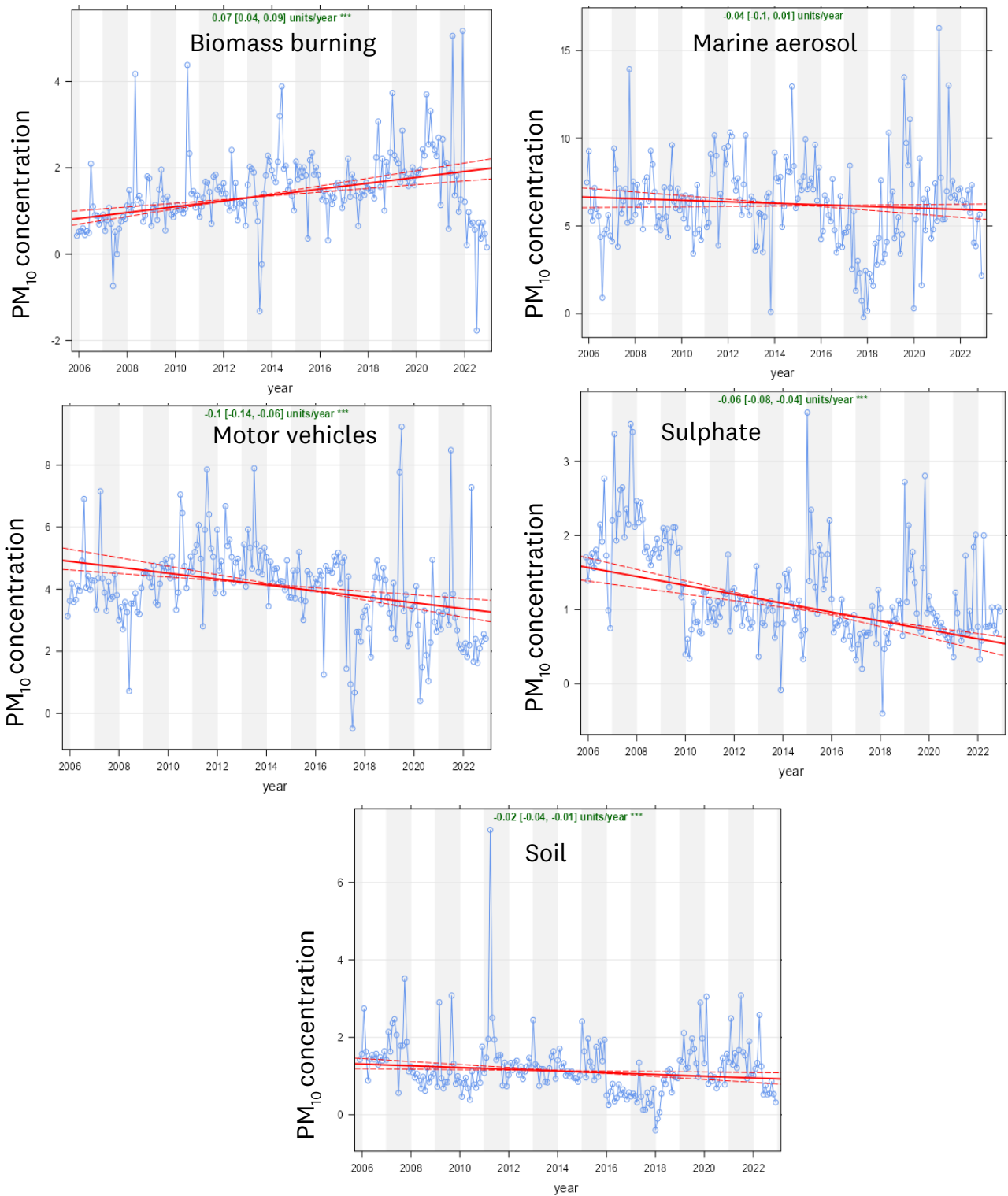


**Figure 14.** Long-term trends in the PM<sub>10</sub> source contributions at the Takapuna site. The plot shows the deseasonalised monthly mean concentrations.

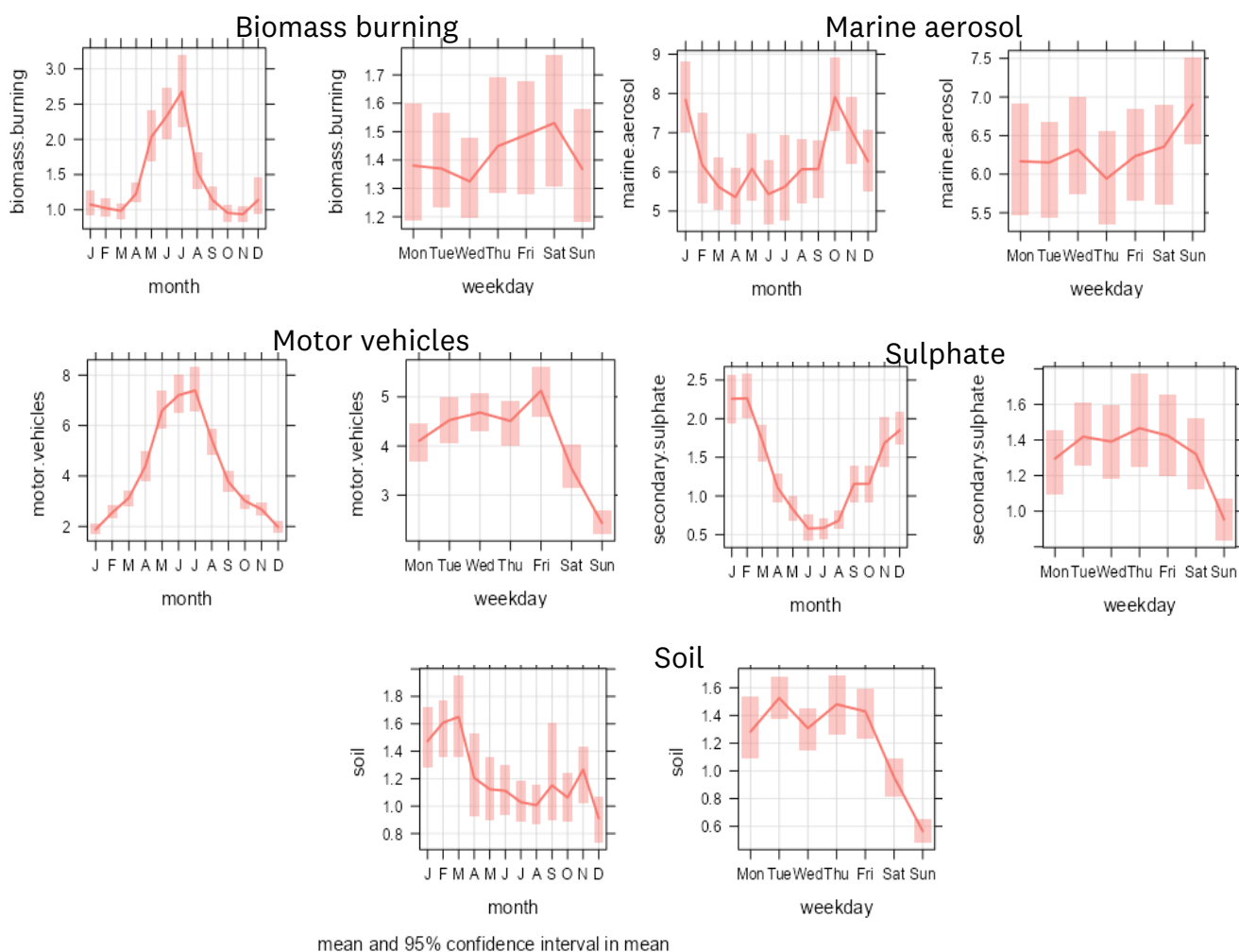


**Figure 15.** Temporal variations in PM<sub>10</sub> source contributions at the Takapuna site (the shaded bars are the 95<sup>th</sup> percentile confidence limits in the mean).

Emissions from the soil source accounted for 8% of the PM<sub>10</sub> data and significantly contributed to the concentrations of Al, Si, Fe, Ti, Ca, and Mn. The soil source contributions at Takapuna likely included windblown soil, road dust, and dust generated by construction and road works. The highest soil source contributions to PM<sub>10</sub> were predominantly from the northwest and southeast sectors (Figure 13). Contrary to the PM<sub>2.5</sub> source apportionment results (Boamponsem et al. 2024), there was a significant downward trend for the soil PM<sub>10</sub> source factor over the monitoring period (Figure 14).

### 3.2.4 Henderson

PM<sub>10</sub> pollution mainly originates from the southwestern quarter as indicated by Appendix H. The PMF solution for the Henderson site resolved five factors: marine aerosol, motor vehicles, biomass burning, sulphate, and soil. The average source contributions revealed by PMF indicate that

marine aerosol, motor vehicle emissions, sulphate, and biomass burning are the most significant contributors to PM<sub>10</sub> concentrations at the Henderson site with lower contributions from soil. Figure 16 displays the source profiles extracted from the PMF analysis of Henderson site PM<sub>10</sub> data. Time series plot of the sources is given in Appendix I.

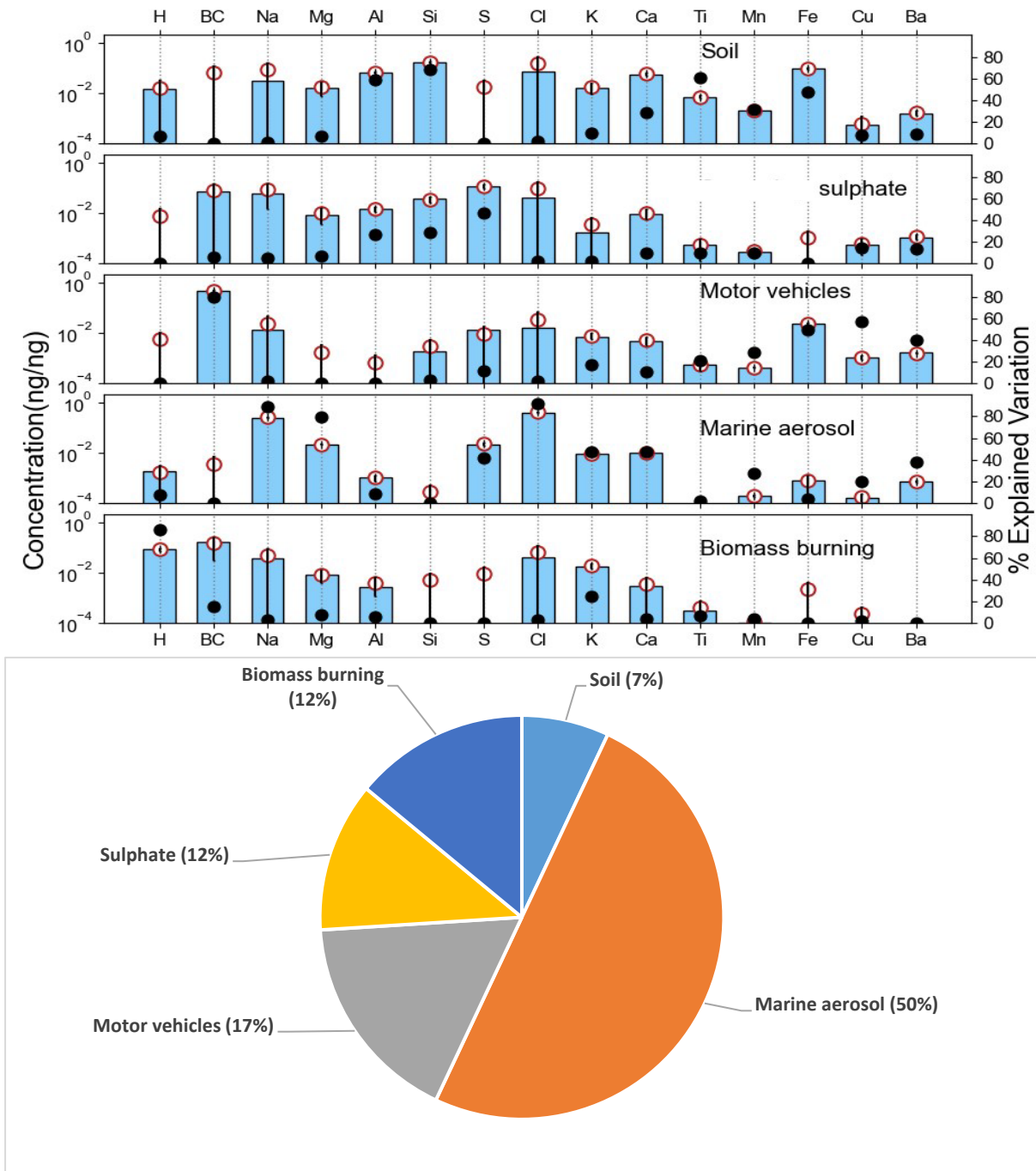


**Figure 16.** Profiles of the sources resolved by the PMF analysis of the Henderson site data collected during 2006-2022. Top plot: The blue bars are the base values, the unfilled red circle lines are the mean fractional displacement (DISP) values, the asymmetric error bars represent the maximum and minimum DISP values. The filled black circle dots represent the % explained variation.



Marine aerosol accounted for 50% of the overall PM<sub>10</sub> average mass concentration, with Na and Cl being the dominant species contributed by this source. Marine aerosol contributions at Henderson mainly originate from the west-southwest and northeast directions (Figure 17), primarily from the Tasman Sea and Pacific Ocean. Like the Queen Street site, a downward trend in the marine aerosol source contributions was observed at the Henderson site (Figure 18). The contribution of the marine aerosol source was highest during the spring months and lowest in winter (Figure 19).

Motor vehicles accounted for 17% of the overall average PM<sub>10</sub> concentration and primarily contributed to BC, Cu, Ti, and Ba. The higher motor vehicle source contributions to PM<sub>10</sub> concentrations in winter are consistent with colder conditions and less efficient combustion (cold-start engine emissions). Motor vehicle emissions from Henderson mainly originate from southeast, likely from the nearby Lincoln Road (Figure 17). There was a significant downward trend in motor vehicles contributions to PM<sub>10</sub> levels over the monitoring period (Figure 18).

Sulphate accounted for 12% of the overall PM<sub>10</sub> average mass concentration, with S, Si, BC, Na, Cl and Al being the dominant species contributed by this source. The contributions here were much smaller than at Queen St. This difference was expected given that easterly flow is a low prevalence direction. The highest per cent of PM<sub>10</sub> sulphate contributions primarily originated from the northwestern sector (Figure 17), likely the result of biogenic sulphate from the oxidation of dimethyl sulphide and dimethyl disulphide (Charlson et al., 1987) similar to what was seen in the Canadian harbours (Anastasopoulos et al., 2023). There was a significant downward trend in the sulphate factor contribution to PM<sub>10</sub> levels at the Henderson site (Figure 18). Like the Queen Street site, seasonal patterns showed that sulphate source concentrations generally have a summer maximum and a winter minimum (Figure 19) suggesting a strong influence of biogenic sulphate from the ocean.

Biomass burning contributed 14% to the overall PM<sub>10</sub> average concentrations, significantly contributing to BC, and K. As with other sites, biomass burning had its highest contributions during winter, likely due to emissions from solid fuel fires for domestic heating. Similar to the Queen Street site, the trend in the contribution of biomass burning since 2018 has been markedly downwards (Figure 18). The apparent reduction in biomass burning emissions at the Henderson and Queen Street sites may be attributed to the use of alternative space-heating technologies such as heat pumps, despite the city's population growth. This was an explicit objective of the Resource Management (National Environmental Standards for Air Quality) Regulations 2004 and

the Building Act 2004 by encouraging cleaner forms of heating and providing installation requirements.

Emissions from soil suspension accounted for 7% of the PM<sub>10</sub> data and substantially contributed to Al, Si, Ti, Ca, Fe, and Mn levels. These contributions are likely the result of road dust, and dust generated by moving vehicles and road works. Short-term road works, construction activities, and demolition near the monitoring site have contributed to this factor. Soil source contributions at Henderson site were highest from the southeast sector, likely originating from the construction and agricultural activity in the Henderson Valley area. There is no significant upward trend for the soil PM<sub>10</sub> source factor over the monitoring period (Figure 18).

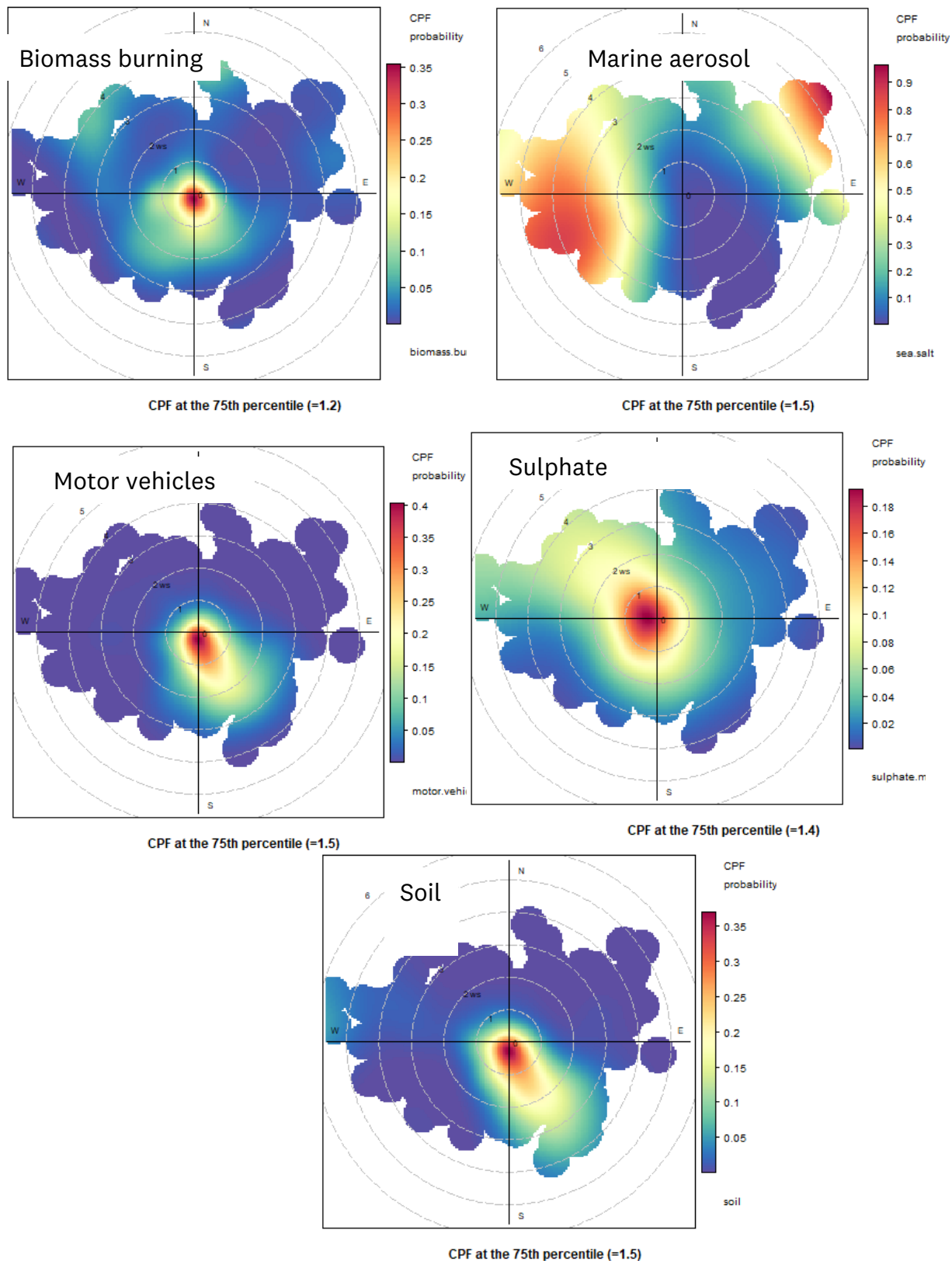


**Figure 17.** CBPF plots for each of the seven factors extracted from the Henderson dataset. Wind speeds are in m/s. Values in the parentheses are the 75th percentile values in  $\mu\text{g}/\text{m}^3$ .

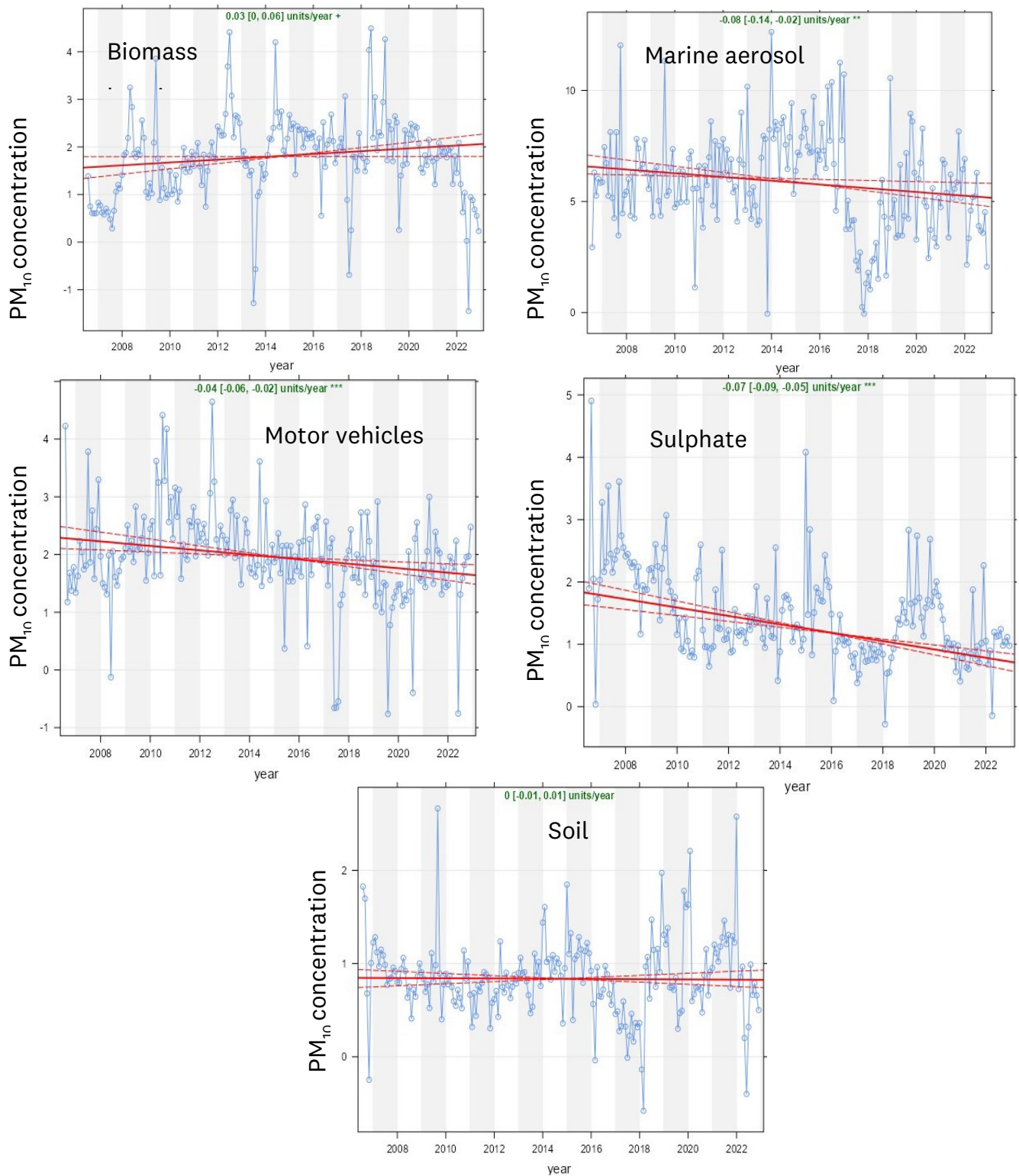


**Figure 18.** Long-term trends in the PM<sub>10</sub> source contributions at the Henderson site. The plot shows the deseasonalised monthly mean concentrations.

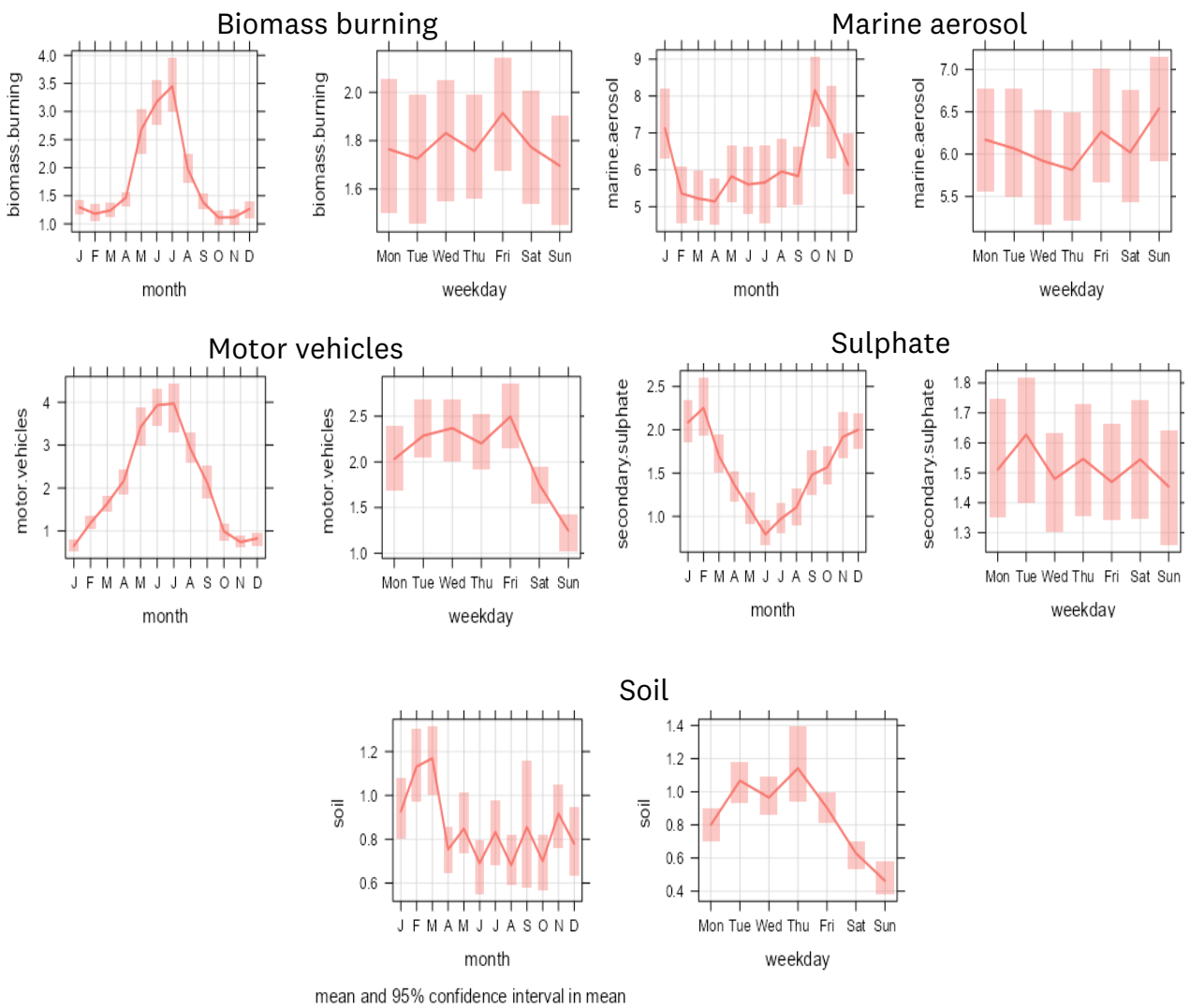


**Figure 19.** Temporal variations in PM<sub>10</sub> source contributions at the Henderson site (the shaded bars are the 95 percentile confidence limits in the mean)

## 4 Conclusions

This study has provided valuable insights into the composition, sources, and trends of PM<sub>10</sub> in Auckland. In line with the findings by Davy et al. (2017), Davy and Trompetter (2020) and Boamponsem et al. (2024), this study identified five sources that are common to all sites. These are marine aerosol, motor vehicles, biomass burning, sulphate, and soil. The marine aerosol component of urban air particulate matter is part of the 'natural' background and therefore a challenge to manage. The soil source was present as a minor contributor at all sites and was largely dependent on the nature of local dust generating activities. Over the 2006-2022 monitoring period, a consistent decrease in PM<sub>10</sub> concentrations was observed across all monitored sites. The decreasing trends of PM<sub>10</sub> is mainly associated with decreases in contributions from the primary anthropogenic PM<sub>10</sub> source, motor vehicle emissions due to improvements in fuel formulation and advancements in engine technology.

Biomass burning was found to contribute significantly to PM<sub>10</sub> during winter months, primarily due to solid fuel fire emissions from residential wood burning for space heating purposes. Stabilisation of biomass burning contributions to PM<sub>10</sub> levels at Queen Street and Henderson is likely due to alternative heating technologies and regulatory measures, despite population growth.

Emissions of particulate matter from ships' engines were found to be directly impacting on the Auckland city centre and the wider region, through the formation of secondary aerosol species from the gaseous combustion products reflective of the high sulphur content of shipping fuels. Sulphate concentrations were highest during spring and summer months and showed a decreasing trend over the monitoring period. This reduction is attributed to fuel formulation regulations that stipulated the introduction of low-sulphur automotive fuels between 2006 and 2010, which led to decreased precursor gases such as SO<sub>2</sub>, primarily from the combustion of sulphur-containing fuels in urban areas.

This source apportionment study in Auckland together with our earlier paper (Boamponsem et al. 2024), have shed light on the main contributors to airborne particulate matter and pollutant gases. This represents the largest source apportionment study undertaken in New Zealand to date and provides key evidence for air quality management and health effects studies in both the Auckland region and New Zealand as a whole.

## 5 References

Agrawal, H., Malloy, Q., Welch, W.A., Miller, J.W., Cocker, D.R., 2008a. In-use gaseous and particulate matter emissions from a modern oceangoing container vessel. *Atmos. Environ.* 42, 5504-5510. <https://doi.org/10.1016/j.atmosenv.2008.02.053>.

Agrawal, H., Welch, W.A., Miller, J.W., Cocker, D.R., 2008b. Emission measurements from a crude oil tanker at sea. *Environ. Sci. Technol.* 42, 7098-7103. <https://doi.org/10.1021/es703102y>.

Agrawal, H., Eden, R., Zhang, X., Fine, P.M., Katzenstein, A., Miller, J.W., Ospital, J., Teffera, S., Cocker III, D.R., 2009. Primary particulate matter from ocean-going engines in the Southern California air basin. *Environ. Sci. Technol.* 43, 5398-5402. <https://doi.org/10.1021/es8035016>.

Agrawal, H., Welch, W.A., Henningsen, S., Miller, J.W., Cocker III, D.R., 2010. Emissions from main propulsion engine on container ship at sea. *J. Geophys. Res.* 115, D23205. <https://doi.org/10.1029/2009JD013346>.

Amato, F., Pandolfi, M., Viana, M., Querol, X., Alastuey, A., and Moreno, T. 2009. Spatial and chemical patterns of PM<sub>10</sub> in road dust deposited in urban environment. *Atmos. Environ.* 43, 1650-1659.

Anastasopoulos, A.T., Hopke, P.K., Sofowote, U.M., Mooibroek, D., Zhang, J.J.Y., Rouleau, M. Peng, H., Sundar, N., 2023. Evaluating the effectiveness of low-sulphur marine fuel regulations at improving urban ambient PM<sub>2.5</sub> air quality: Source apportionment of PM<sub>2.5</sub> at Canadian Atlantic and Pacific coast cities with implementation of the North American Emissions Control Area, *Sci. Total Environ.* 904, 166965.

Ancelet T, Davy PK, Mitschell T, Trompetter WJ, Markwitz A, Weatherburn DC. 2012. Source of particulate matter pollution in a small New Zealand city. *Environ. Sci. Technol.* 46:4767-4774.

Ancelet T, Davy PK, Trompetter WJ, Markwitz A, Weatherburn DC 2014. Sources and transport of particulate matter on an hourly time-scale during the winter in a New Zealand urban valley. *Urban Clim* 10:644-655.

Atkinson, W.R., Fuller, W.G., Anderson, R.H., Harrison, M.R., Armstrong, M.B., 2010. Urban ambient particle metrics and health: a time-series analysis. *Epidemiology*, 21 (4), 501-511.

Barry, B., Trompetter, W. J., Davy, P. K., and Markwitz, A. 2012. Recent developments in the air particulate research capability at the New Zealand Ion Beam Analysis Facility. *International Journal of PIXE*, 22, 121-130.

Bergamaschi, L., Rizzio, E., Profumo, A., and Gallorini, M. 2005. Determination of trace elements by INAA in urban air particulate matter and transplanted lichens. *Journal of Radioanalytical and Nuclear Chemistry*, 263(3), 745-750.

Boamponsem, L. K., De Freitas, C. R., and Williams, D. 2017. Source apportionment of air pollutants in the Greater Auckland Region of New Zealand using receptor models and elemental levels in the lichen, *Parmotrema reticulatum*. *Atmospheric Pollution Research*, 8(1), 101-113.

Boamponsem, L. K., P. K. Hopke and P. K. Davy 2024. Long-term trends and source apportionment of fine particulate matter (PM<sub>2.5</sub>) and gaseous pollutants in Auckland, New Zealand. *Atmospheric Environment* 322: 120392.

Cavanagh, J.-A. E., Trought, K., Brown, L., and Duggan, S. 2009. Exploratory investigation of the chemical characteristics and relative toxicity of ambient air particulates from two New Zealand cities. *Science of the Total Environment*, 407(18), 5007-5018.

Carslaw, D. C. 2012. The openair manual – open-source tools for analyzing air pollution data. Manual for version 0.7-0, King's College London.

Carslaw, D. C. 2015. The openair manual – open-source tools for analyzing air pollution data. Manual for version 1.1-4, King's College London.



Carslaw, D. C. 2018. Package “openair”. Tools for the analysis of air pollution data. Available from <http://davidcarslaw.github.io/openair/>, Accessed date: October 2023.

Carslaw, David, and K. Ropkins. 2012. Openair – An R Package for Air Quality Data Analysis. *Environmental Modelling & Software* 27-28, January, 52-61.

Charlson, R.J., Lovelock, J.E., Andreae, M.O., Warren, S.G., 1987. Oceanic phytoplankton, atmospheric sulfur, cloud albedo and climate. *Nature* 326, 655-661.

Crimmins, P. 2017. Quantifying Black Carbon Emissions from Residential Wood Burning by a Combination of Bottom-Up and Top-Down Approaches, Auckland: University of Auckland MSc Thesis.

Crimmins, P., Dirks, K., and Salmond, J. 2019. The challenge of quantifying black carbon emissions: A case study from Auckland, New Zealand. *Air Quality and Climate Change*, 53(1), 12-18.

Croft, D.P., Zhang, W., Lin, S., Thurston, S.W., Hopke, P.K., Van Wijngaarden, E., Squizzato, S., Masiol, M., Utell, M.J., Rich, D.Q. 2020. The associations between source specific particulate matter and of respiratory infections in New York state adults. *Environ. Sci. Technol.* 54, 975-984.

Dai, Q., Ding, J., Song, C., Liu, B., Bi, X., Wu, J., Zhang, Y., Feng, Y., Hopke, P.K. 2021. Changes in source contributions to particle number concentrations after the COVID-19 outbreak: Insights from a dispersion normalized PMF. *Science of The Total Environment*, 759, 143548.

Davy, P. K., Ancelet, T., Trompetter, W. J., and Markwitz, A. 2017. Source apportionment and trend analysis of air particulate matter in the Auckland region. Prepared by the Institute of Geological and Nuclear Sciences Ltd, GNS Science for Auckland Council. Auckland Council technical report, TR2017/001.

Davy, P. K., Trompetter, W. J. 2020. Composition, sources and long-term trends for Auckland air particulate matter: summary report. Lower Hutt (NZ): GNS Science. 32 p. Consultancy Report 2019/151.

Davy, P. K., Trompetter, W. J. 2021. Elemental analysis results for air particulate matter collected in Auckland, 2006-2021. Lower Hutt (NZ): GNS Science. 57p. Consultancy Report 2021/45.

de Jesus, A.L., Thompson, H., Knibbs, L.D., Kowalski, M., Cyrus, J., Niemi, J.V., Kousa, A., Timonen, H., Luoma, K., Petäjä, T., Beddows, D. 2020. Long-term trends in PM<sub>2.5</sub> mass and particle number concentrations in urban air: The impacts of mitigation measures and extreme events due to changing climates. *Environmental Pollution*, 263, 114500.

Dehghani, M.H., Hopke, P.K., Asghari, F.B., Mohammadi, A.A., Yousefi, M. 2020. The effect of the decreasing level of Urmia Lake on particulate matter trends and attributed health effects in Tabriz, Iran. *Microchemical Journal*, 153, 104434.

Edwards, J. D., Ogren, J. A., Weiss, R. E., and Charlson, R. J. 1983. Particulate Air Pollutants: A Comparison of British “Smoke” with Optical Absorption Coefficient and Elemental Carbon Concentration. *Atmos. Environ.* 17: 2337-2341.

EFCA. 2019. Ambient ultrafine particles: evidence for policymakers. White paper prepared by the ‘Thinking outside the box’ team, European Federation of Clean Air and Environmental Protection Associations, Version 1, 25 October 2019. Available at [https://efca.net/files/WHITE%20PAPER-UFP%20evidence%20for%20policy%20makers%20\(25%20OCT\).pdf](https://efca.net/files/WHITE%20PAPER-UFP%20evidence%20for%20policy%20makers%20(25%20OCT).pdf)

Forouzanfar, M.H., Afshin, A., Alexander, L.T., Anderson, H.R., Bhutta, Z.A., Biryukov, S., et al. 2016. Global, regional, and national comparative risk assessment of 79 behavioural, environmental and occupational, and metabolic risks or clusters of risks, 1990-2015: a systematic analysis for the Global Burden of Disease Study 2015. *Lancet* 388, 1659-1724.

Global Burden of Disease (GBD), 2020. Global burden of 87 risk factors in 204 countries and territories, 1990-2019: a systematic analysis for the Global Burden of Disease Study 2019. *Lancet* 396, 1223-1249.

Gianini, M., Fischer, A., Gehrig, R., Ulrich, A., Wichser, A., Piot, C., Hueglin, C. 2012. Comparative source apportionment of PM<sub>10</sub> in Switzerland for 2008/2009 and 1998/1999 by positive matrix factorization. *Atmos. Environ.* 54, 149-158.

Health Effects Institute. 2024. State of Global Air 2024. Special Report. Health Effects Institute. Boston, USA.

Health Effects Institute (HEI). 2018. State of global air 2018. Special Report. Health Effects Institute, Boston, USA.

Hopke PK 2016. Review of receptor modelling methods for source apportionment. *J. Air Waste Manage. Assoc.* 66, 237-259.

Hopke, P. K. 2009. Theory and application of atmospheric source apportionment. *Developments in Environmental Science*, 9, 1-33.

Hopke, P. K., Hidy, G. 2022. Changing Emissions Results in Changed PM<sub>2.5</sub> Composition and Health Impacts. *Atmosphere* 13, 193. <https://doi.org/10.3390/atmos13020193>.

Hopke, P.K., Dai, Q., Li, L., Feng, Y., 2020a. Global review of recent source apportionments for airborne particulate matter. *Sci. Total Environ.* 740, 140091. <https://doi.org/10.1016/j.scitotenv.2020.140091>.

Hopke, P. K., Croft, D., Zhang, W., Shao, L., Masiol, M., Squizzato, S., Thurston, S.W., van Wijngaarden, E., Utell, M.J., Rich, D.Q. 2020b. Changes in the hospitalization and ED visit rates for respiratory diseases associated with source-specific PM<sub>2.5</sub> in New York State from 2005 to 2016. *Environ. Res.* 181, 108912.

Hovorka, J., Pokorná, P., Hopke, P.K., Křůmal, K., Mikuška, P., Pířová, M. 2015. Wood combustion, a dominant source of winter aerosol in residential district in proximity to a large automobile factory in Central Europe. *Atmospheric Environment*, 113, 98-107.

International Maritime Organization (IMO), 2021. IMO2020 fuel oil sulphur limit – cleaner air, healthier planet. Available online at: <https://www.imo.org/en/MediaCentre/PressBriefings/pages/02-IMO-2020.aspx>

Janssen, N.A., Hoek, G., et al. 2011. Black carbon as an additional indicator of the adverse health effects of airborne particles compared with PM<sub>10</sub> and PM<sub>2.5</sub>. *Environ. Health Perspect.* 119 (12), 1691-1699.

Kuschel et al. 2022. Health and air pollution in New Zealand 2016 (HAPINZ 3.0): Volume 1 – Finding and implications. Report prepared by G. Kuschel, J. Metcalfe, S. Sridhar, P. Davy, K. Hastings, K. Mason, T. Denne, J. Berentson-Shaw, S. Bell, S. Hales, J. Atkinson and A. Woodward for Ministry for the Environment, Ministry of Health, Te Manatū Waka Ministry of Transport and Waka Kotahi NZ Transport Agency, March 2022.  
<https://environment.govt.nz/assets/publications/HAPINZ/HAPINZ-3.0-Findings-and-implications.pdf> (Accessed: 20 July 2022)

Laura E. Revell, Nicholas J. Edkins, Abhijith U. Venugopal, Yusuf A. Bhatti, Kathleen M. Kozyniak, Perry K. Davy, Gerda Kuschel, Elizabeth Somervell, Catherine Hardacre and Guy Coulson (26 Feb 2024): Marine aerosol in Aotearoa New Zealand: implications for air quality, climate change and public health, *Journal of the Royal Society of New Zealand*, DOI: 10.1080/03036758.2024.2319753

Maleki, M., Anvari, E., Hopke, P.K., Noorimotlagh, Z., Mirzaee, S.A. 2021. An updated systematic review on the association between atmospheric particulate matter pollution and prevalence of SARS-CoV-2. *Environmental research*, 195, 110898.

Metcalfe, J., Wickham, L., and Sridhar, S. 2018. Auckland air emissions inventory 2016 – home heating. Prepared by Emission Impossible Ltd for Auckland Council. Auckland Council technical report, TR2018/018

Ministry for the Environment and Statistics New Zealand (MfE and Stats NZ). 2021. New Zealand's Environmental Reporting Series: Our air 2021. Available at [www.environment.govt.nz](http://www.environment.govt.nz), (Accessed: 18 January 2022)

Moghadamnia, M.T., Ardalani, A., Mesdaghinia, A., Keshtkar, A., Naddafi, K., Yekaninejad, M.S. 2017. Ambient temperature and cardiovascular mortality: a systematic review and meta-analysis. *Peer J* 5, 3574.

Moreno T, Kojima T, Amato A, Lucarelli F, de la Rosa J, Calzolari G, Nava S, Chiari M, Alastuey A, Querol X, Gibbons W 2013. Daily and hourly chemical impact of springtime transboundary aerosols on Japanese air quality. *Atmos Chem Phys* 13:1411-1424.

Norris, G., and Rachele, D. 2014. EPA Positive Matrix Factorization (PMF) 5.0 Fundamentals and User Guide. U.S. Environmental Protection Agency, Washington. [https://www.epa.gov/sites/default/files/2015-02/documents/pmf\\_5.0\\_user\\_guide.pdf](https://www.epa.gov/sites/default/files/2015-02/documents/pmf_5.0_user_guide.pdf) (Accessed: 20 January 2021)

NZ Ministry of Transport. 2018. Annual fleet statistics 2018. <https://www.transport.govt.nz/assets/Uploads/Report/The-NZ-Vehicle-Fleet-Report-2018-web-v2.pdf> (Accessed: 1 November 2023).

Paatero, P., Tapper, U. 1993. Analysis of different modes of factor analysis as least squares fit problems. *Chemom. Intell. Lab. Syst.* 18, 183 - 194.

Paatero, P., Eberly, S., Brown, S. G., and Norris, G. A. 2014. Methods for estimating uncertainty in factor analytic solutions, *Atmos. Meas. Tech.*, 7, 781-797, doi:10.5194/amt-7-781-2014.

Patel, H., Talbot, N., Salmond, J., Dirks, K., Xie, S., and Davy, P. 2020. Implications for air quality management of changes in air quality during lockdown in Auckland (New Zealand) in response to the 2020 SARS-CoV-2 epidemic. *Science of the Total Environment*, 746, 141129.

Patel, H., Davy, P., Tollemache, C., Talbot, N., Salmond, J., and Williams, D. E. 2024. Evaluating the efficacy of targeted traffic management interventions: A novel methodology for determining the composition of particulate matter in urban air pollution hotspots. *Science of the total environment*, 951, 175414.

Pirsaheb, M., Sharafi, K., Hopke, P.K., Hadei, M., Shahsavani, A. 2020. Carcinogenic risks of particulate matter during Middle Eastern dust events and normal days. *Atmospheric Pollution Research*, 11(9), 1566-1571.

Pokorná, P., Leoni, C., Schwarz, J., Ondráček, J., Ondráčková, L., Vodička, P., Zíková, N., Moravec, P., Bendl, J., Klán, M., Hovorka, J. 2020. Spatial-temporal variability of aerosol sources based on chemical composition and particle number size distributions in an urban settlement influenced by metallurgical industry. *Environmental Science and Pollution Research*, 27, 38631-38643.

Pope III, C.A., Ezzati, M., et al. 2009. Fine-particulate air pollution and life expectancy in the United States. *N. Engl. J. Med.* 360 (4), 376-386.

Potukuchi, S., Wexler, A.S. 1995. Identifying solid-aqueous-phase transitions in atmospheric aerosols. II. Acidic solutions. *Atmos. Environ.* 29 (22), 3357-3364.

Smodiš, B. 2007. Investigation of trace element atmospheric pollution by nuclear analytical techniques at a global scale: harmonised approaches supported by the IAEA. *Journal of environmental management*, 85(1), 121-128.

Song, C., He, J., Wu, L., Jin, T., Chen, X., Li, R., Ren, P., Zhang, L., Mao, H. 2017. Health burden attributable to ambient PM<sub>2.5</sub> in China. *Environ. Pollut.* 223, 575-586.

Stanimirova, I., Rich, D.Q., Russell, A.G., Hopke, P.K. 2023. A long-term, dispersion normalized PMF source apportionment of PM<sub>2.5</sub> in Atlanta from 2005 to 2019. *Atmospheric Environment*, 312, 120027.

Tao, Y., Huang, W., Huang, X., Zhong, L., Lu, S., Li, Y., et al. 2011. Estimated acute effects of ambient ozone and nitrogen dioxide on mortality in the Pearl River Delta of Southern China. *Environ. Health Perspect.* 120, 393-398.

Tobías, A., Rivas, I., Reche, C., Alastuey, A., Rodríguez, S., Fernandez-Camacho, R., Sanchez de La Campa, A.M., de La Rosa, J., Sunyer, J., Querol, X., 2018. Short-term effects of ultrafine particles on daily mortality by primary vehicle exhaust versus secondary origin in three Spanish cities. *Environ. Int.* 111, 144-151.

Trompetter, W., Markwitz, A., and Davy, K. 2005. Air particulate research capability at the New Zealand Ion Beam Analysis Facility using PIXE and IBA Techniques. *International Journal of PIXE* 15 (3&4), 249-255.

Uria-Tellaetxe, I., Carslaw, D. C. 2014. Conditional bivariate probability function for source identification. *Environmental Modelling & Software* 59, 1-9.

<https://doi.org/10.1016/j.envsoft.2014.05.002>

Viana, M., Pandolfi, M., Minguillón, M., Celades, I. 2008. Inter-comparison of receptor models for PM source apportionment: case study in an industrial area. *Atmospheric Environment*, 42(16), 3820-3832.

Vestenius, M., Leppänen, S., Anttila, P., Kyllönen, K., Hatakka, J., Hellen, H., and Hakola, H. 2011. Background concentrations and source apportionment of polycyclic aromatic hydrocarbons in south-eastern Finland. *Atmos. Environ.* 45, 3391-3399.

World Health Organization. 2021. WHO global air quality guidelines: particulate matter (PM<sub>2.5</sub> and PM<sub>10</sub>), ozone, nitrogen dioxide, sulfur dioxide and carbon monoxide. Available at <https://apps.who.int/iris/handle/10665/345329> (Accessed: 18 January 2022).

World Health Organization. 2018. Burden of disease from ambient air pollution for 2016, version 2. April 2018. Geneva: World Health Organization  
[https://www.who.int/airpollution/data/AAP\\_BoD\\_results\\_May2018\\_final.pdf?ua=1](https://www.who.int/airpollution/data/AAP_BoD_results_May2018_final.pdf?ua=1) accessed 20 November 2021.

Xie, S., Crimmins, P., Metcalfe, J., Sridhar, S., and Wickham, L. 2019. Auckland Air Emissions Inventory 2016 – road vehicle emissions. Prepared by Emission Impossible Ltd for Auckland Council. Auckland Council technical report, TR2017/024.

Yin, G., Liu, C., Hao, L., Chen, Y., Wang, W., Huo, J., Zhao, Q., Zhang, Y., Duan, Y., Fu, Q., Chen, R., Kan, H., 2019. Associations between size-fractionated particle number concentrations and COPD mortality in Shanghai, China. *Atmos. Environ.* 214, 116875.

## **6 Acknowledgements**

We express our gratitude to the Auckland Council for their continued support and funding for the source apportionment programme. We are grateful to Dr. W. J. Trompetter and the dedicated laboratory team at GNS Science for their invaluable assistance and guidance. We extend special thanks to the air quality team at Watercare Services Ltd, and Mote Ltd for their collaboration in the collection of particulate matter samples. Many thanks to Jacqueline Lawrence-Sansbury and Gustavo Olivares Pino for their helpful comments in the development of this report.



## 7 Appendices

### 8 Appendix A: PM<sub>10</sub> concentration trends – 2006 to 2022

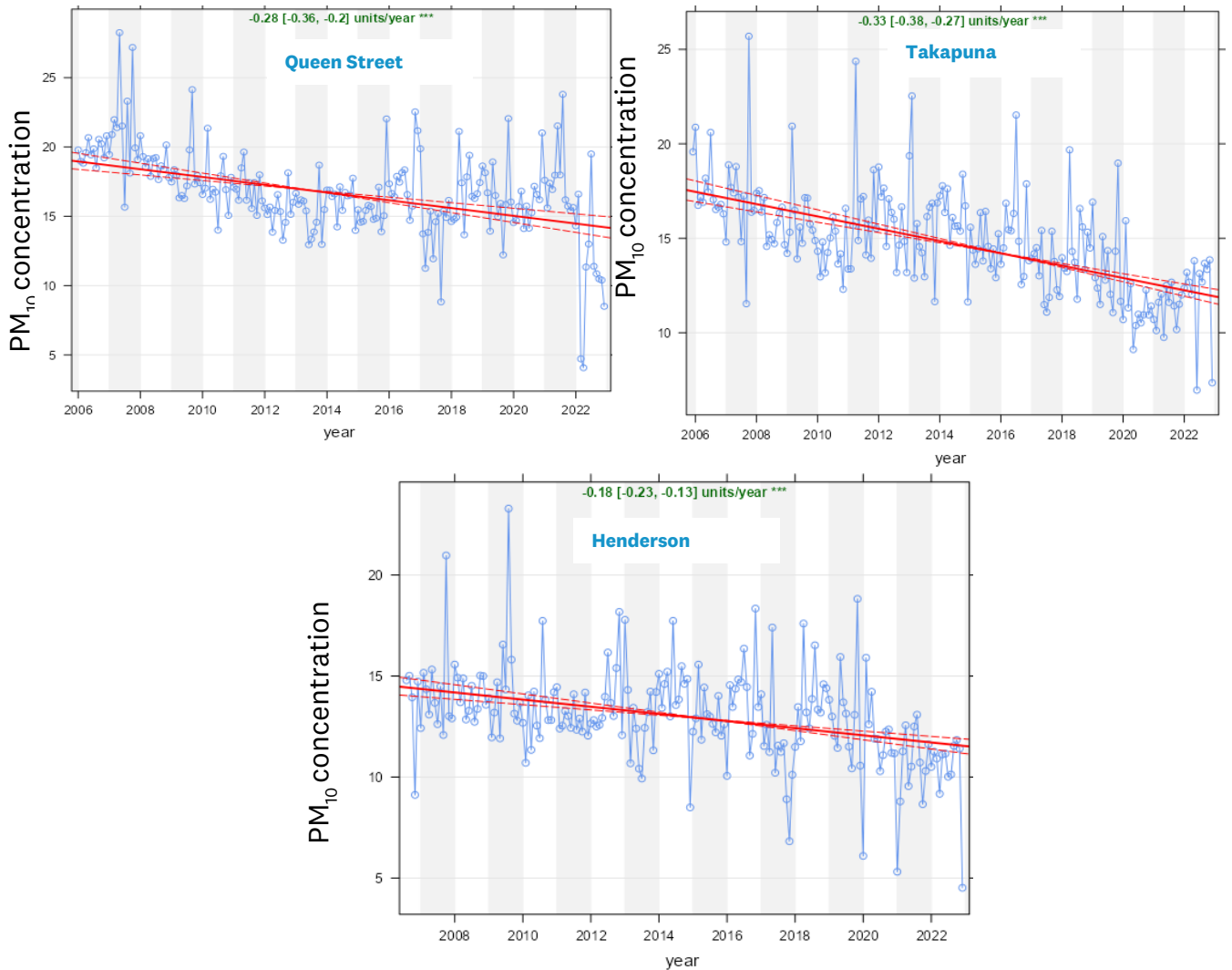


**Figure A1.** Long-term trends in the PM<sub>10</sub> concentrations (Gravimetric) at the Queen Street, Takapuna, and Henderson. The plot shows the deseasonalised monthly mean concentrations.

## 9 Appendix B: PM<sub>10</sub> elemental concentrations box plot

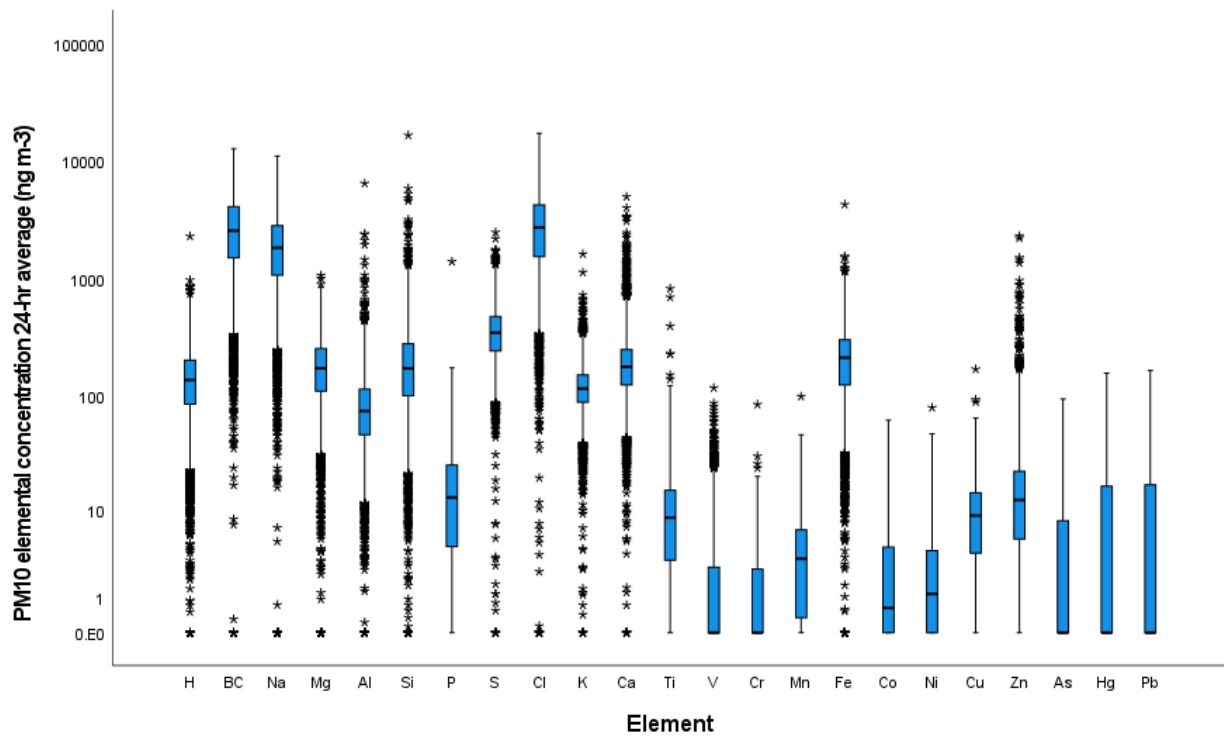


**Figure A2.** Box and whisker plot of PM<sub>10</sub> elemental concentrations across all monitoring sites (y-axis in logarithmic scale). Boxes represent 25<sup>th</sup> (bottom of the box) and 75<sup>th</sup> (top of box) percentile, central line through the box is the median, bars outside the box (whiskers) represent the 1.5× interquartile range, \* markers are the means, and circles are outliers.

# 10 Appendix C: Box plot of all sources identified

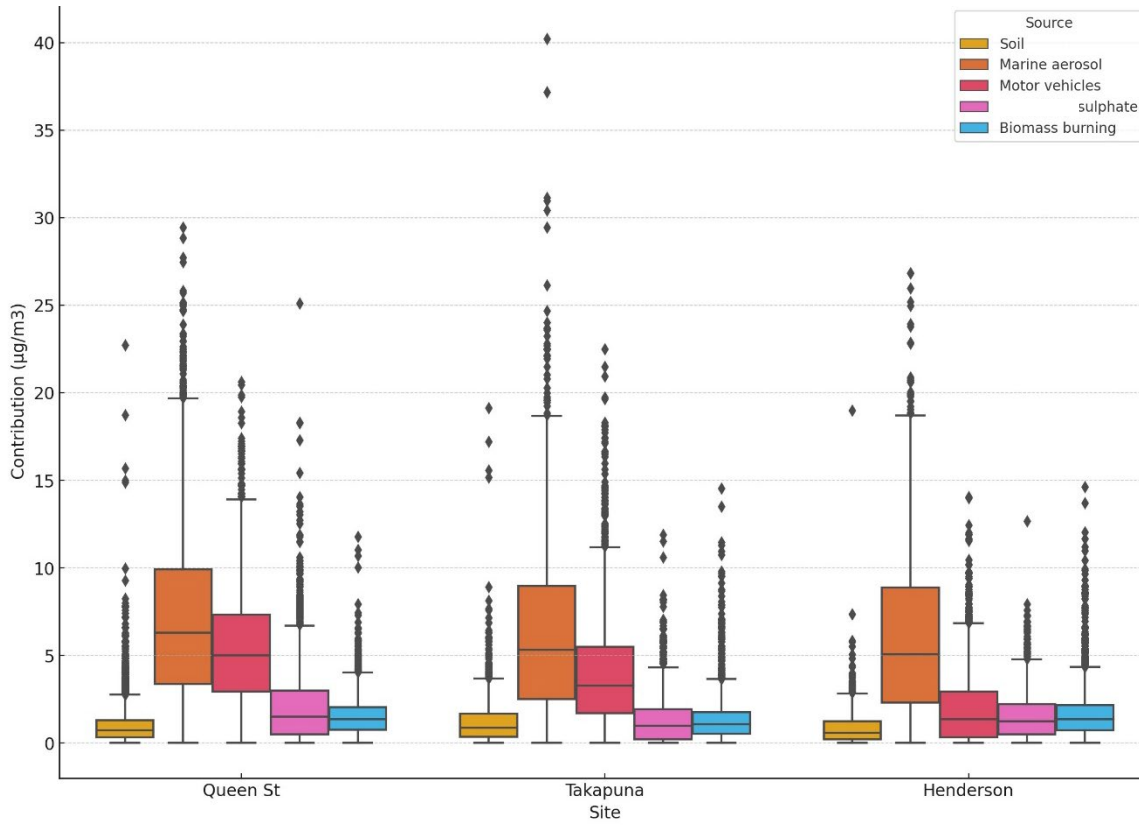
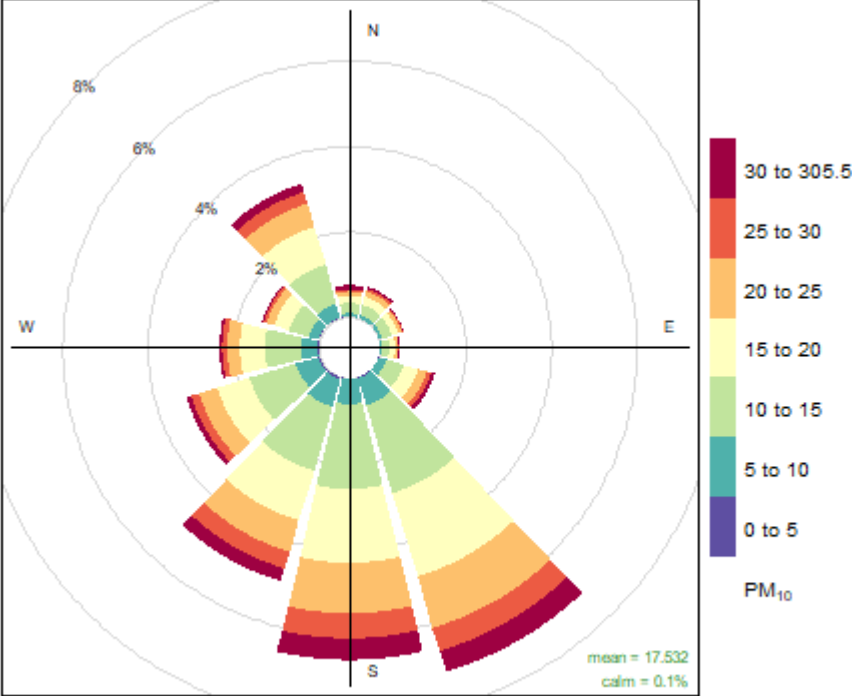


**Figure A3.** Boxplot of the PM<sub>10</sub> gravimetric mean concentrations and the source contributors across the four sites. Boxes represent 25<sup>th</sup> (bottom of the box) and 75<sup>th</sup> (top of box) percentile, central line through the box is the median, bars outside the box (whiskers) represent the 1.5× interquartile range, × markers are the means, and circles are outliers.

# 11 Appendix D: Pollution roses for Queen Street



Frequency of counts by wind direction (%)

**Figure A4.** PM<sub>10</sub> pollution rose for Queen Street

## 12 Appendix E. Source profiles time series – Queen Street

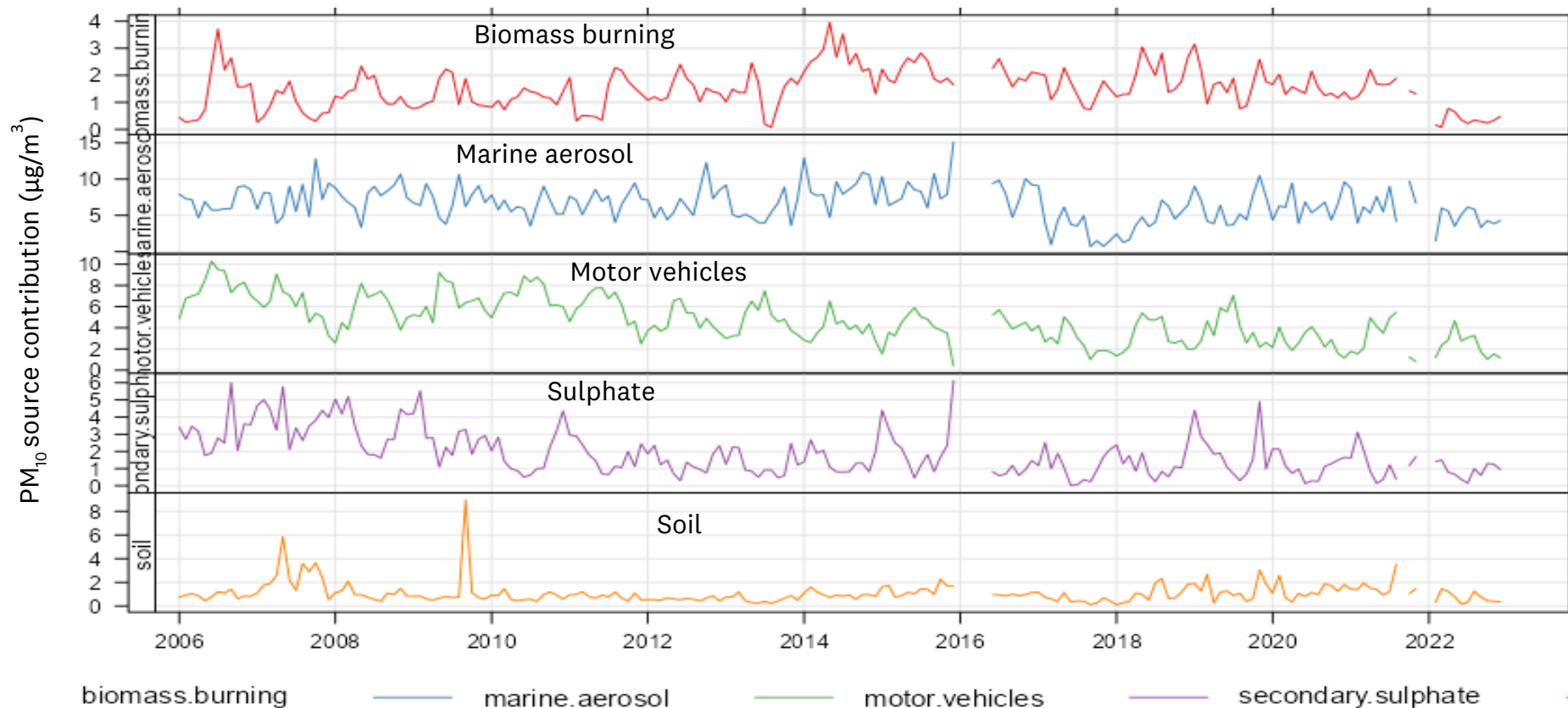
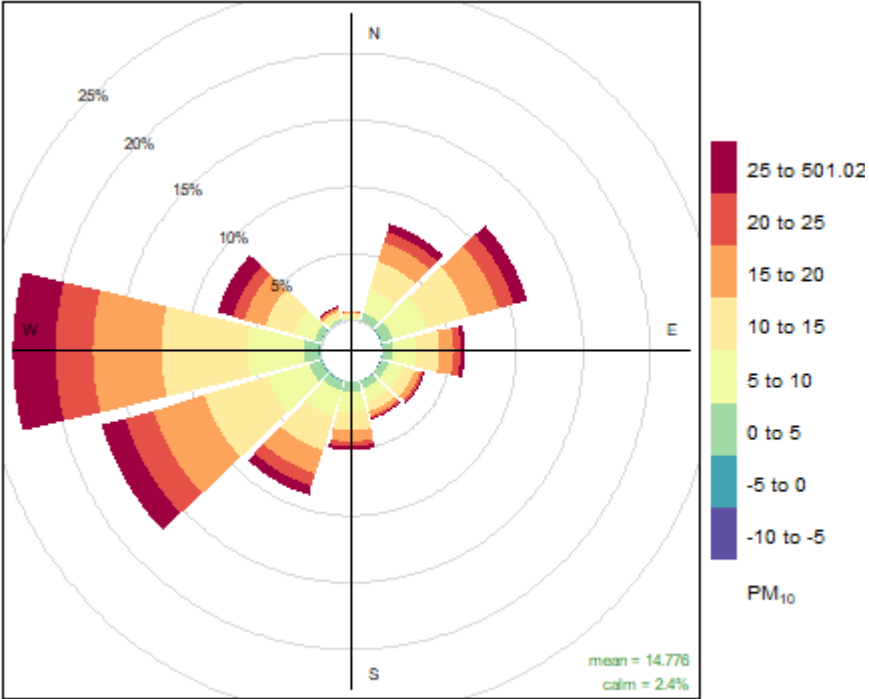


**Figure A5.** Time series of contributions of the factors resolved using the PMF analysis (Queen Street site)

# 13 Appendix F: Pollution rose for Takapuna site



Frequency of counts by wind direction (%)

Figure A6. PM<sub>10</sub> pollution roses for Takapuna site

## 14 Appendix G: Source profiles time series – Takapuna site

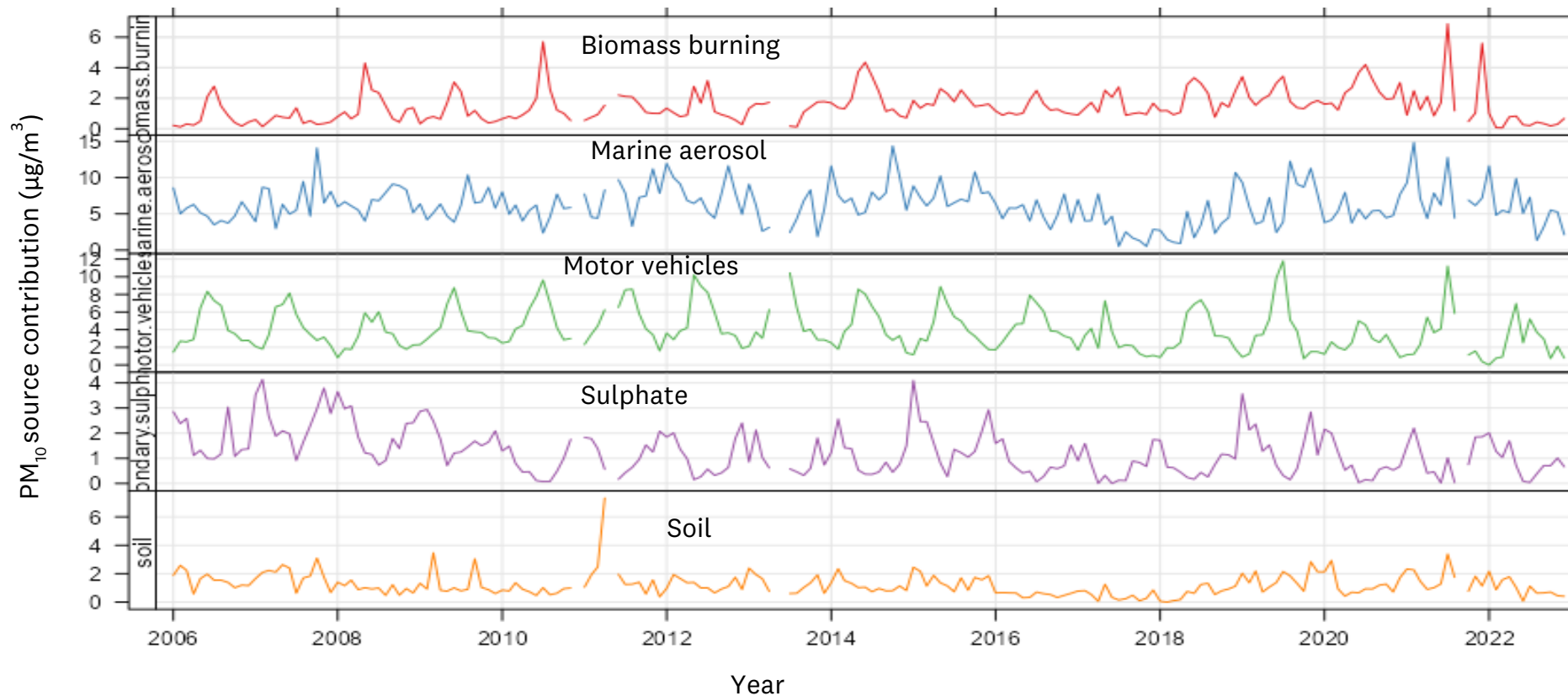
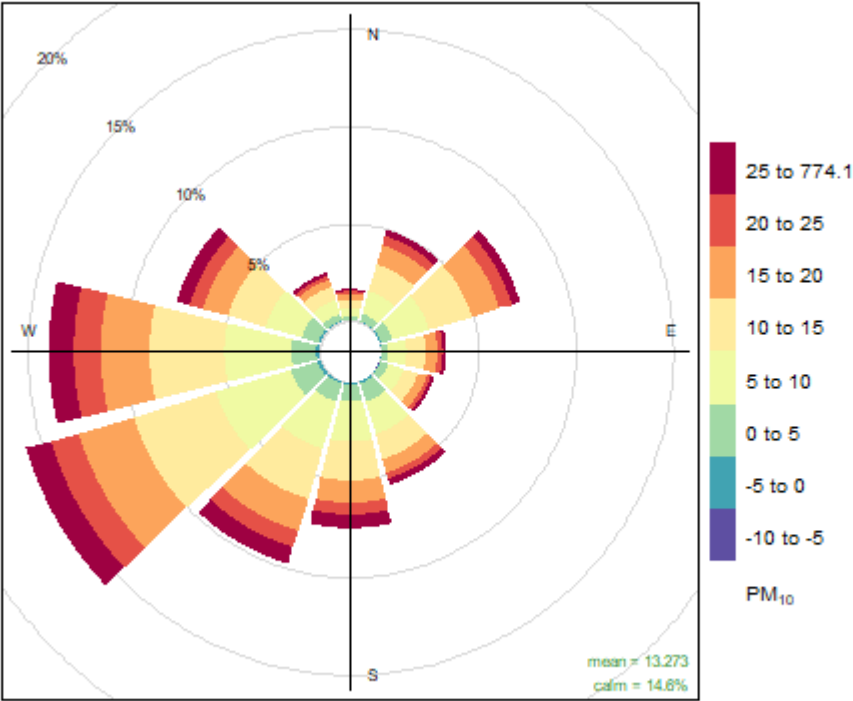


**Figure A7.** Time series of contributions of the factors resolved using the PMF analysis (Takapuna site)

# 15 Appendix H: Pollution roses for Henderson



Frequency of counts by wind direction (%)

Figure A8. PM<sub>10</sub> pollution roses for Henderson



## 16 Appendix I: Source profiles time series plot – Henderson site

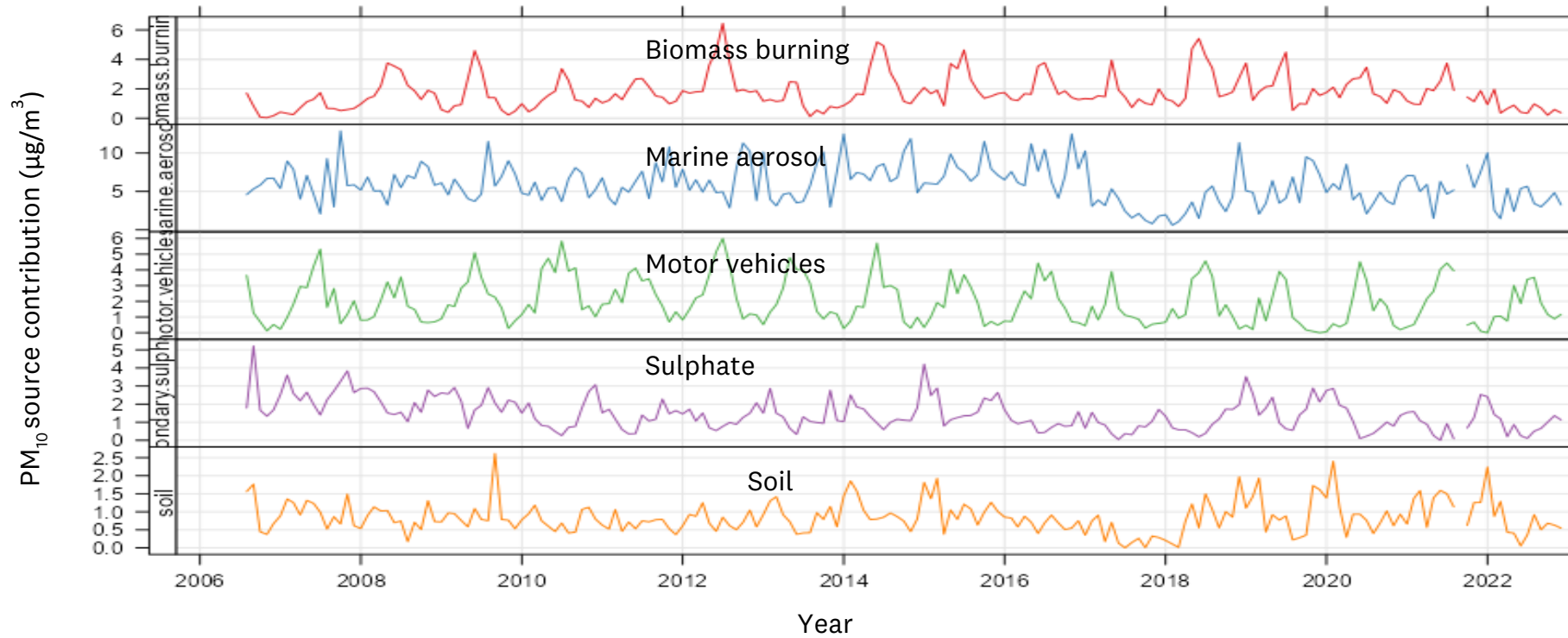


**Figure A9.** Time series of contributions of the factors resolved using the PMF analysis (Henderson site)

## 17 Appendix J: Source profiles time series plot – All sites

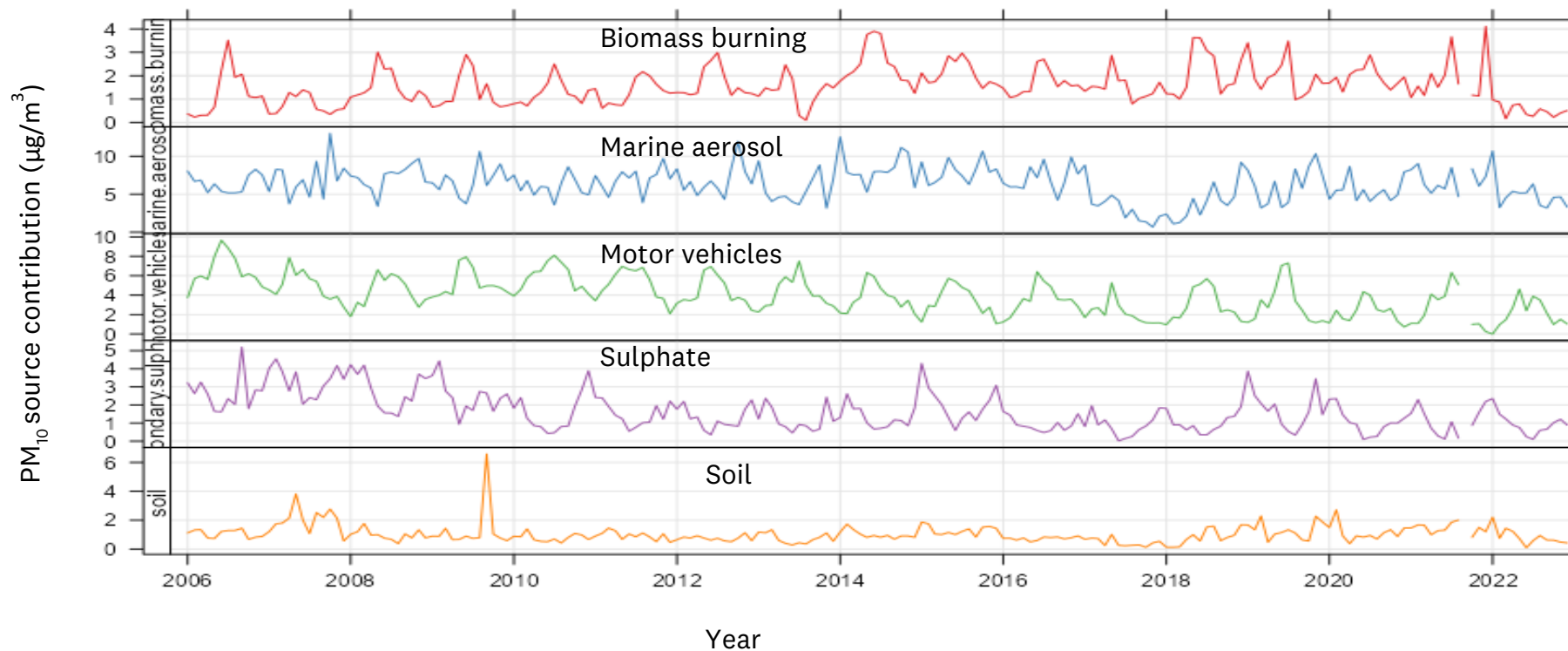


**Figure A10.** Time series of contributions of the factors resolved using the PMF analysis (Auckland)



Find out more: email

[EnvironmentalData@aucklandcouncil.govt.nz](mailto:EnvironmentalData@aucklandcouncil.govt.nz)  
or visit [knowledgeauckland.org.nz](https://knowledgeauckland.org.nz) and  
[aucklandcouncil.govt.nz](https://aucklandcouncil.govt.nz)

